incorporated substantially into severely injured arteries. And many studies have suggested that EPCs are involved in the early repair of injured arteries (*31*). Because it is generally accepted that insulin resistance enhances vascular lesion formation, it may be possible that EPCs have little effect on neointimal formation under normal conditions but play an important role in the repair of injured arteries under pathological conditions such as diabetes and insulin resistance. Alternatively, these results may suggest that EPCs do not contribute to the repair of vascular injury in the acute or subacute stage of BI.

Insulin has various effects on VSMCs. Trovati *et al.* (*32*) reported that insulin increased cGMP and cAMP levels in VSMC. Because these cyclic nucleotides are reported to inhibit VSMC growth (*33*), insulin resistance may enhance VSMC proliferation after BI. In contrast, it was also reported that insulin itself has a weak growth-promoting effect on VSMC (*34*, *35*) and augments the growth-promoting effect of platelet-derived growth factor. In this case, insulin resistance may have a favorable effect on vasculature. In endothelial cells, insulin stimulates NO production (*35*). NO inhibits many of the processes associated with atherosclerosis. It is known that NO inhibits VSMC growth, suggesting that insulin resistance of endothelial cells may reduce NO production, resulting in the enhancement of VSMC growth. The reduction of NO level may enhance expression of tumor necrosis factor-α and monocyte chemoattractant protein-1 (*36*), which are believed to accelerate atherogenesis. Because of the complex nature of the direct insulin action on blood vessels as indicated above, it is difficult to determine whether or not improvement of insulin resistance by combination treatment of Olm and Pra contributed to the reduction of neointimal formation in our model. However, it is generally believed that insulin resistance and hyperinsulinemia enhance atherogenesis (*37*), suggesting that the improvement of insulin resistance by Olm and Pra treatment may play a role in the inhibition of neointimal formation.

In conclusion, we showed in the present study that the combination of Olm and Pra has beneficial effects on vascular remodeling after injury and insulin sensitivity in rats fed a fructose-rich diet. These data suggest that the combination of ARB and statin may be recommended for patients with CHD and insulin resistance. Because these drugs did not change BP or blood lipid levels, it is reasonable to assume that these beneficial effects of ARBs and statins were independent of BP- or lipid-lowering properties.

References

1. Stumvoll M, Goldstein BJ, van Haeften TW: Type 2 diabetes: principles of pathogenesis and therapy. *Lancet* 2005; **365**: 1333–1346.
2. Grundy SM: Metabolic syndrome: connecting and reconciling cardiovascular and diabetes worlds. *J Am Coll Cardiol* 2006; **47**: 1093–1100.
3. Ford ES: Risks for all-cause mortality, cardiovascular disease, and diabetes associated with the metabolic syndrome: a summary of the evidence. *Diabetes Care* 2005; **28**: 1769–1778.
4. de Gasparo M, Catt KJ, Inagami T, Wright JW, Unger T: International union of pharmacology. XXIII. The angiotensin II receptors. *Pharmacol Rev* 2000; **52**: 415–472.
5. Pfeffer MA, McMurray JJ, Velazquez EJ, *et al*: Valsartan, captopril, or both in myocardial infarction complicated by heart failure, left ventricular dysfunction, or both. *N Engl J Med* 2003; **349**: 1893–1906.
6. Pfeffer MA, Swedberg K, Granger CB, *et al*: Effects of candesartan on mortality and morbidity in patients with chronic heart failure: the CHARM-Overall programme. *Lancet* 2003; **362**: 759–766.
7. Barnett AH, Bain SC, Bouter P, *et al*: Angiotensin-receptor blockade *versus* converting-enzyme inhibition in type 2 diabetes and nephropathy. *N Engl J Med* 2004; **351**: 1952–1961.
8. Dahlof B, Sever PS, Poulter NR, *et al*: Prevention of cardiovascular events with an antihypertensive regimen of amlodipine adding perindopril as required *versus* atenolol adding bendroflumethiazide as required, in the Anglo-Scandinavian Cardiac Outcomes Trial-Blood Pressure Lowering Arm (ASCOT-BPLA): a multicentre randomised controlled trial. *Lancet* 2005; **366**: 895–906.
9. Wilt TJ, Bloomfield HE, MacDonald R, *et al*: Effectiveness of statin therapy in adults with coronary heart disease. *Arch Intern Med* 2004; **164**: 1427–1436.
10. Jain MK, Ridker PM: Anti-inflammatory effects of statins: clinical evidence and basic mechanisms. *Nat Rev Drug Discov* 2005; **4**: 977–987.
11. Horiuchi M, Cui TX, Li Z, *et al*: Fluvastatin enhances the inhibitory effects of a selective angiotensin II type 1 receptor blocker, valsartan, on vascular neointimal formation. *Circulation* 2003; **107**: 106–112.
12. Li Z, Iwai M, Wu L, *et al*: Fluvastatin enhances the inhibitory effects of a selective AT1 receptor blocker, valsartan, on atherosclerosis. *Hypertension* 2004; **44**: 758–763.
13. Nishikawa H, Miura S, Shimomura H, *et al*: Combined treatment with statin and angiotensin-receptor blocker after stenting as a useful strategy for prevention of coronary restenosis. *J Cardiol* 2005; **45**: 107–113.
14. Morawietz H, Erbs S, Holtz J, *et al*: Endothelial protection, AT1 blockade and cholesterol-dependent oxidative stress: the EPAS trial. *Circulation* 2006; **114**: I296–I301.
15. Togashi N, Ura N, Higashiura K, Murakami H, Shimamoto K: Effect of TNF-alpha–converting enzyme inhibitor on insulin resistance in fructose-fed rats. *Hypertension* 2002; **39**: 578–580.
16. Kim S, Izumi Y, Izumiya Y, Zhan Y, Taniguchi M, Iwao H: Beneficial effects of combined blockade of ACE and AT1 receptor on intimal hyperplasia in balloon-injured rat artery. *Arterioscler Thromb Vasc Biol* 2002; **22**: 1299–1304.
17. Li C, Yang CW, Park JH, *et al*: Pravastatin treatment attenuates interstitial inflammation and fibrosis in a rat model of chronic cyclosporine-induced nephropathy. *Am J Physiol Renal Physiol* 2004; **286**: F46–F57.
18. Tokunou T, Shibata R, Kai H, *et al*: Apoptosis induced by inhibition of cyclic AMP response element–binding protein

in vascular smooth muscle cells. *Circulation* 2003; **108**: 1246–1252.
19. Simper D, Wang S, Deb A, *et al*: Endothelial progenitor cells are decreased in blood of cardiac allograft patients with vasculopathy and endothelial cells of noncardiac origin are enriched in transplant atherosclerosis. *Circulation* 2003; **108**: 143–149.
20. D'Angelo G, Elmarakby AA, Pollock DM, Stepp DW: Fructose feeding increases insulin resistance but not blood pressure in Sprague-Dawley rats. *Hypertension* 2005; **46**: 806–811.
21. Okada K, Hirano T, Ran J, Adachi M: Olmesartan medoxomil, an angiotensin II receptor blocker ameliorates insulin resistance and decreases triglyceride production in fructose-fed rats. *Hypertens Res* 2004; **27**: 293–299.
22. Yamakawa T, Tanaka S, Numaguchi K, *et al*: Involvement of Rho-kinase in angiotensin II–induced hypertrophy of rat vascular smooth muscle cells. *Hypertension* 2000; **35**: 313–318.
23. Begum N, Sandu OA, Ito M, Lohmann SM, Smolenski A: Active Rho kinase (ROK-alpha) associates with insulin receptor substrate-1 and inhibits insulin signaling in vascular smooth muscle cells. *J Biol Chem* 2002; **277**: 6214–6222.
24. Martin G, Duez H, Blanquart C, *et al*: Statin-induced inhibition of the Rho-signaling pathway activates PPARalpha and induces HDL apoA-I. *J Clin Invest* 2001; **107**: 1423–1432.
25. Morikawa-Futamatsu K, Adachi S, Maejima Y, *et al*: HMG-CoA reductase inhibitor fluvastatin prevents angiotensin II–induced cardiac hypertrophy *via* Rho kinase and inhibition of cyclin D1. *Life Sci* 2006; **79**: 1380–1390.
26. Negre-Aminou P, van Vliet AK, van Erck M, van Thiel GC, van Leeuwen RE, Cohen LH: Inhibition of proliferation of human smooth muscle cells by various HMG-CoA reductase inhibitors; comparison with other human cell types. *Biochim Biophys Acta* 1997; **1345**: 259–268.
27. Weiss RH, Ramirez A, Joo A: Short-term pravastatin mediates growth inhibition and apoptosis, independently of Ras, *via* the signaling proteins p27Kip1 and P13 kinase. *J Am Soc Nephrol* 1999; **10**: 1880–1890.
28. Walter DH, Rittig K, Bahlmann FH, *et al*: Statin therapy accelerates reendothelialization: a novel effect involving mobilization and incorporation of bone marrow–derived endothelial progenitor cells. *Circulation* 2002; **105**: 3017–3024.
29. Yamamoto E, Yamashita T, Tanaka T, *et al*: Pravastatin enhances beneficial effects of olmesartan on vascular injury of salt-sensitive hypertensive rats, *via* pleiotropic effects. *Arterioscler Thromb Vasc Biol* 2007; **27**: 556–563.
30. Tanaka K, Sata M, Hirata Y, Nagai R: Diverse contribution of bone marrow cells to neointimal hyperplasia after mechanical vascular injuries. *Circ Res* 2003; **93**: 783–790.
31. Strehlow K, Werner N, Berweiler J, *et al*: Estrogen increases bone marrow–derived endothelial progenitor cell production and diminishes neointima formation. *Circulation* 2003; **107**: 3059–3065.
32. Trovati M, Anfossi G: Influence of insulin and of insulin resistance on platelet and vascular smooth muscle cell function. *J Diabetes Complications* 2002; **16**: 35–40.
33. Koyama H, Bornfeldt KE, Fukumoto S, Nishizawa Y: Molecular pathways of cyclic nucleotide–induced inhibition of arterial smooth muscle cell proliferation. *J Cell Physiol* 2001; **186**: 1–10.
34. Hsueh WA, Law RE: Insulin signaling in the arterial wall. *Am J Cardiol* 1999; **84**: 21J–24J.
35. Zeng G, Quon MJ: Insulin-stimulated production of nitric oxide is inhibited by wortmannin. Direct measurement in vascular endothelial cells. *J Clin Invest* 1996; **98**: 894–898.
36. Aizawa T, Wei H, Miano JM, Abe J, Berk BC, Yan C: Role of phosphodiesterase 3 in NO/cGMP-mediated antiinflammatory effects in vascular smooth muscle cells. *Circ Res* 2003; **93**: 406–413.
37. Bloomgarden ZT: Inflammation, atherosclerosis, and aspects of insulin action. *Diabetes Care* 2005; **28**: 2312–2319.

Inhibition of Rac1-Derived Reactive Oxygen Species in Nucleus Tractus Solitarius Decreases Blood Pressure and Heart Rate in Stroke-Prone Spontaneously Hypertensive Rats

Masatsugu Nozoe, Yoshitaka Hirooka, Yasuaki Koga, Yoji Sagara, Takuya Kishi, John F. Engelhardt, Kenji Sunagawa

Abstract—Reactive oxygen species (ROS) in the brain are thought to contribute to the neuropathogenesis of hypertension by enhancing sympathetic nervous system activity. The nucleus tractus solitarius (NTS), which receives afferent input from baroreceptors, has an important role in cardiovascular regulation. reduced nicotinamide-adenine dinucleotide phosphate oxidase is thought to be a major source of ROS in the NTS. Rac1 is a small G protein and a key component of reduced nicotinamide-adenine dinucleotide phosphate oxidase. The role of Rac1-derived ROS in the NTS in cardiovascular regulation of hypertension is unknown. Therefore, we examined whether inhibition of Rac1 in the NTS decreases ROS generation, thereby reducing blood pressure in stroke-prone spontaneously hypertensive rats (SHRSPs). The basal Rac1 activity level in the NTS was greater in SHRSPs than in Wistar-Kyoto rats. Inhibition of Rac1, induced by transfecting adenovirus vectors encoding dominant-negative Rac1 into the NTS, decreased blood pressure, heart rate, and urinary norepinephrine excretion in SHRSPs but not in Wistar-Kyoto rats. Inhibition of Rac1 also reduced nicotinamide-adenine dinucleotide phosphate oxidase activity and ROS generation. In addition, Cu/Zn-superoxide dismutase activity in the NTS of SHRSPs was decreased compared with that of Wistar-Kyoto rats, despite the increased ROS generation. Overexpression of Cu/Zn-superoxide dismutase in the NTS decreased blood pressure and heart rate in SHRSPs. These results indicate that the activation of Rac1 in the NTS generates ROS via reduced nicotinamide-adenine dinucleotide phosphate oxidase in SHRSPs, and this mechanism might be important for the neuropathogenesis of hypertension in SHRSPs. (***Hypertension*. 2007;50:62-68.**)

Key Words: blood pressure ■ heart rate ■ sympathetic nervous system ■ hypertension ■ brain

There is accumulating evidence that reactive oxygen species (ROS) in the cardiovascular regulatory nuclei in the brain have a crucial role in blood pressure regulation in hypertension via modulating the sympathetic nervous system.[1–5] Reduced nicotinamide-adenine dinucleotide phosphate [NAD(P)H] oxidase is a major source of ROS in hypertension[6] and has a critical role in generating ROS in the brain.[2,5,7] Rac1 is a small G protein that is an important signaling molecule involved in integrating intracellular transduction pathways toward NAD(P)H oxidase activation.[2,8,9] Rac1 requires lipid modifications to migrate from the cytosol to the plasma membrane, which is a necessary step for activating the ROS-generating NAD(P)H oxidase enzyme system.[8,9]

The nucleus tractus solitarius (NTS) in the brain stem has an important role in cardiovascular regulation.[10–16] The NTS receives afferent input from baroreceptors and chemoreceptors[12] and has reciprocal interconnections with other nuclei involved in central autonomic regulation.[17] In addition, the essential NAD(P)H oxidase subunit $gp91^{phox}$ is present in somatodendritic and axonal profiles that contain angiotensin II (Ang II) subtype 1 receptors in the NTS, and Ang II increases ROS generation via NAD(P)H oxidase in NTS neurons in vitro.[7] The role of Rac1 and its derived ROS in the NTS in cardiovascular regulation of hypertension in vivo, however, is not known. Therefore, the aim of the present study was to determine the effects of the inhibition of Rac1 in the NTS on cardiovascular regulation of hypertension in the awake state. For this purpose, we transfected an adenovirus vector dominant-negative Rac1 into the NTS of stroke-prone spontaneously hypertensive rats (SHRSPs) and compared the effects with those in normotensive Wistar-Kyoto rats (WKYs).

Methods

An expanded Methods section is available in the online data supplement at http://hyper.ahajournals.org.

Received January 24, 2007; first decision February 12, 2007; revision accepted April 27, 2007.

From the Department of Cardiovascular Medicine (M.N., Y.H., Y.K., Y.S., T.K., K.S.), Kyushu University Graduate School of Medical Sciences, Fukuoka, Japan; and the Department of Anatomy and Cell Biology (J.F.E.), University of Iowa, Iowa City.

Correspondence to Yoshitaka Hirooka, Department of Cardiovascular Medicine, Kyushu University Graduate School of Medical Sciences, 3-1-1 Maidashi, Higashi-ku, Fukuoka 812-8582, Japan. E-mail hyoshi@cardiol.med.kyushu-u.ac.jp

Hypertension **is available at http://www.hypertensionaha.org** **DOI: 10.1161/HYPERTENSIONAHA.107.087981**

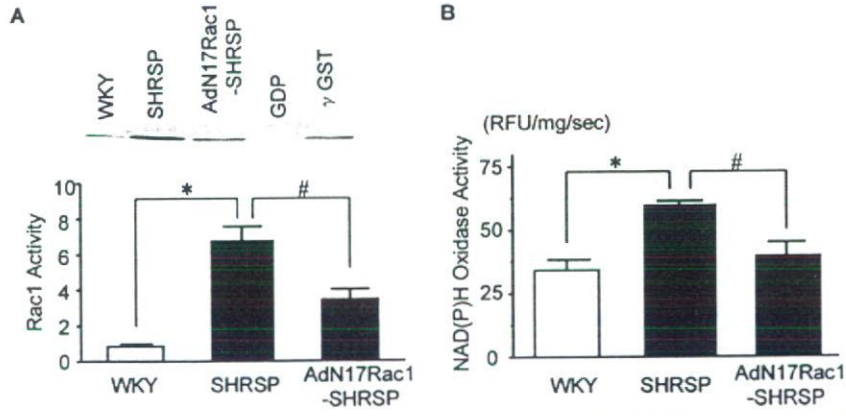

Figure 1. Rac1 and NAD(P)H oxidase activities are elevated in SHRSPs but not in WKYs. A, Rac1 activity in the NTS. The top panel shows a representative Western blot of Rac1-GTP bound to glutathione *S*-transferase–Pak1. Quantification of Rac1–GTP activity expressed as the relative ratio to control (WKYs), which was assigned a value of 1 (bottom). Rac1 activity in the NTS of SHRSPs was significantly increased compared with that of WKYs. Furthermore, dominant-negative Rac1 gene transfer significantly attenuated Rac1 activity in the NTS of SHRSPs. Lysates incubated with GDP or γ-GTP served as negative and positive controls, respectively (n=4 for each; *$P<0.01$ vs WKY; #$P<0.05$ vs SHRSP). B, NAD(P)H oxidase activity evaluated by lucigenin chemiluminescence in the NTS. NAD(P)H-dependent superoxide production was significantly higher in SHRSPs than in WKYs. Furthermore, dominant-negative Rac1 gene transfer significantly attenuated NAD(P)H oxidase activity in the NTS of SHRSPs (WKY rats=34.2±4.1; SHRSP=59.6±1.5; AdN17Rac1-transfected SHRSP=39.2±5.8 relative fluorescence units/mg/s; n=5 for each; *$P<0.05$ vs WKY; #$P<0.05$ vs SHRSP).

Animals and General Procedures

Male SHRSPs and WKYs (280 to 340 g; 14 to 18 weeks old) were obtained from SLC Japan (Hamamatsu, Japan). The study was reviewed and approved by the Committee of Ethics of Animal Experiments, Kyushu University Graduate School of Medical Sciences, and was conducted according to the Guidelines for Animal Experiments of Kyushu University.

Rac1 Activation Assays

Rac1 activity can be monitored by its interaction with p21-activated kinase (PAK), which only occurs when Rac1 is active.[8] We used a Rac1 Activation kit (Upstate Biotechnology) to evaluate Rac1 activity in the NTS.

NAD(P)H-Dependent Superoxide Production

NAD(P)H-dependent superoxide production in the NTS was measured by lucigenin luminescence.[8,18,19] A luminescence assay was performed in a balanced salt solution buffer containing 5 μmol/L of lucigenin (Sigma) using a luminescence reader (Berthold Technology). The reaction was started by adding 100 μmol/L of β-NAD(P)H (Sigma) as the substrate.

In Vivo Gene Transfer Into the NTS

We used adenoviral vectors encoding dominant-negative HA-tagged Rac1 (AdN17Rac1),[2] human Cu/Zn-superoxide dismutase (SOD; AdCu/ZnSOD),[2,20,21] and β-galactosidase (AdLacZ). The vectors were constructed in the Gene Transfer Core Laboratory at the University of Iowa. We transfected AdN17Rac1, AdCu/ZnSOD, and AdLacZ into the NTS as described previously.[10,11] A telemetry system (DATA Sciences International) was used to measure mean blood pressure (MBP) and heart rate (HR).[1,3,10,11] On day 7 after gene transfer, we calculated the 24-hour urinary norepinephrine excretion as an indicator of sympathetic nerve activity.[1,3,10,11]

Analysis of Gene Expression

To confirm the expression and localization of gene transfer in the NTS, we performed immunohistochemical staining for human Cu/Zn-SOD and β-galactosidase. To identify the cell types that were transfected by the adenovirus used in the present study, we performed double immunohistochemical staining for β-galactosidase and a neuronal marker (NeuN; Chemicon International Inc).[22] Western blot analysis was performed using rabbit anti-SOD-1 polyclonal IgG (1:10 000, Santa Cruz Biotechnology), mouse anti-hemagglutinin (HA) monoclonal IgG (1:10 000, Sigma), or rabbit anti-β tubulin polyclonal IgG (1:10 000, Santa Cruz Biotechnology).

In Situ Detection of Superoxide

Brain superoxide anion levels were estimated by dihydroethidium (DHE) staining.[3,5] Coronal sections (10 μm) were incubated for 10 minutes with the O_2^- specific fluorogenic probe DHE (1 μmol/L, Sigma) at 37°C.

Thiobarbituric Acid–Reactive Substances

We examined thiobarbituric acid-reactive substance (TBARS) levels in the NTS as an indicator of oxidative stress, as described previously.[1,3]

Measurement of SOD Activity

Cu/Zn-SOD activity was assayed by monitoring the inhibition of the rate of xanthine/xanthine oxidase–mediated reduction of cytochrome *c*, as described previously.[1]

Statistical Analysis

All of the values were expressed as the mean±SEM. $P<0.05$ was considered significant.

Results

Rac1/NAD(P)H Oxidase Pathway Is Activated in the NTS of SHRSPs

Rac1-GTP levels were assessed as an index of Rac1 activation using a glutathione *S*-transferase–PAK pull-down assay. These studies revealed that Rac1 activity in the NTS of SHRSPs was significantly higher than in the NTS of WKYs (Figure 1A). Consistent with increased Rac1 activation, NAD(P)H-dependent superoxide production was also significantly higher in the NTS from SHRSPs than in the NTS from WKYs (Figure 1B). Gene transfer of AdN17Rac1 into the NTS of SHRSPs suppressed both Rac1/PKA binding (Figure 1A) and NAD(P)H oxidase activity (Figure 1B).

Effect of Rac1 Inhibition and Cu/Zn-SOD by Adenovirus-Mediated Gene Transfer

Western blot analysis of HA-tag, a marker of AdN17Rac1, was performed on tissue samples taken from rats on days 0,

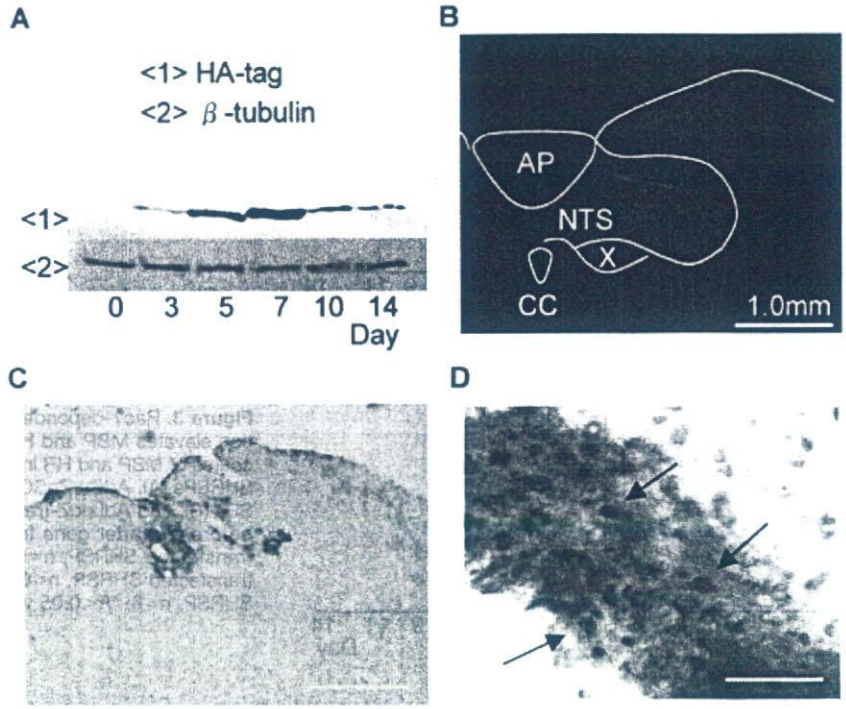

Figure 2. Target gene expression in the NTS using recombinant adenovirus. A, To confirm the gene expression and time course of dominant-negative Rac1 in the NTS, we performed Western blot analysis of HA-tag, a marker of AdN17Rac1, on tissue samples taken from rats on days 0, 3, 5, 7, 10, and 14 after gene transfer. We examined 3 rats at each day, and the figure shows representative images. The expression level of HA-tag was significantly increased and peaked on day 7 after AdN17Rac1 transfection. B, Laser scanning microscopy images of a section of medulla, stained with anti-human Cu/Zn-SOD antibody on day 7 after gene transfer (high intensity, visualized using a fluorescein isothiocyanate–conjugated fluorescence probe). Staining was observed locally in the NTS (AP indicates area postrema; X, dorsal motor nucleus of vagus; CC, central canal; bar=1.0 mm). C, 5-bromo-4-chloro-3-indolyl β-D-galactoside staining on day 7 after gene transfer was localized in the NTS (bar=1.0 mm). D, To identify the cell types that were transfected by the adenovirus used in the present study, we performed double immunohistochemical staining for β-galactosidase and a NeuN. Some NeuN-positive cells expressed β-galactosidase protein, although NeuN-negative cells also expressed β-galactosidase (bar=50 μm; arrows indicate NeuN-positive cells).

3, 5, 7, 10, and 14 after gene transfer (n=3 per day), and representative images are shown in Figure 2A. The HA-tag expression level was significantly increased and peaked on day 7 after AdN17Rac1 transfection. We performed immunohistochemistry to examine the localization and distribution of adenoviral-mediated gene transfer. Immunohistochemical analysis on day 7 after gene transfer revealed localized human Cu/Zn-SOD (Figure 2B) or β-galactosidase gene expression (Figure 2C) in the NTS. Double staining of β-galactosidase and NeuN confirmed that some NeuN-positive cells expressed β-galactosidase protein, although NeuN-negative cells also expressed β-galactosidase protein (Figure 2D). AdN17Rac1-transfected SHRSPs exhibited a significant decrease in MBP and HR (Figure 3A). MBP and HR did not change in AdLacZ-transfected SHRSPs (Figure 3C). Urinary norepinephrine excretion measured on day 7 after gene transfer was significantly decreased in AdN17Rac1-transfected SHRSPs relative to that in non-treated SHRSPs (Figure 4A). In addition, overexpression of Cu/Zn-SOD in the NTS of SHRSPs decreased MBP, HR (Figure 3B), and urinary norepinephrine excretion (Figure 4A). In contrast, AdN17Rac1 and AdCu/ZnSOD transfection into the NTS of WKYs did not affect MBP, HR (Figure S1), or urinary norepinephrine excretion (Figure 4B).

Oxidative Stress in the NTS

Confocal analysis of DHE fluorescence was used to estimate superoxide levels in the NTS. We examined 4 groups (WKY, SHRSP, AdN17Rac1-transfected SHRSP, and AdCu/ZnSOD-transfected SHRSP; n=5 for each), and representative images are shown in Figure 5A. There was a significant increase in DHE fluorescence in sections that contained the NTS of SHRSPs compared with sections of the NTS of WKYs. Furthermore, DHE fluorescence in the NTS was significantly attenuated in both AdN17Rac1-transfected SHRSPs and AdCu/ZnSOD-transfected SHRSPs (Figure 5A). TBARS levels were also significantly higher in the NTS of SHRSPs than in the NTS of WKYs (Figure 5B). Gene transfer of either AdN17Rac1 or AdCu/ZnSOD suppressed TBARS levels in the NTS (Figure 5B), suggesting that the TBARS increase was the result of enhanced superoxide generation.

Expression and Activity of Cu/Zn-SOD in the NTS of SHRSPs

Western blot analysis revealed that the expression of a ≈17-kDa isoform of rat Cu/Zn-SOD protein in the NTS was decreased in SHRSPs compared with WKYs (Figure 6A). There was also significantly less total SOD activity (5.9±0.3 versus 4.9±0.1 U/mg; $P<0.05$; n=5) and Cu/Zn-SOD activ-

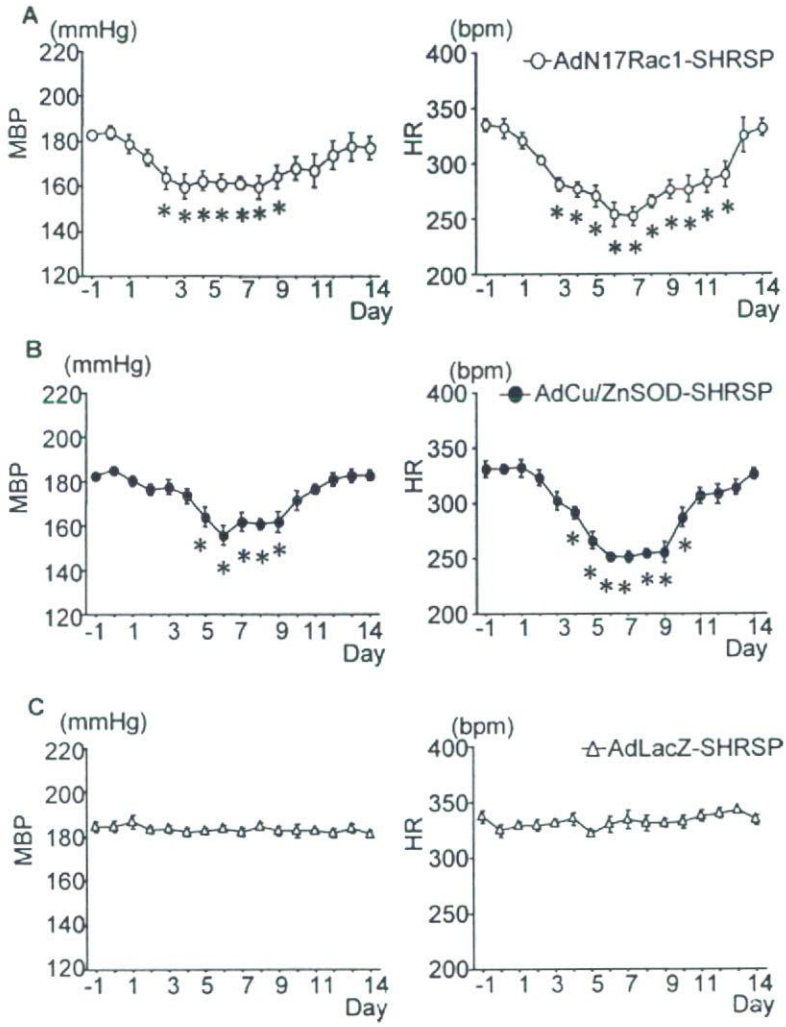

Figure 3. Rac1-dependent superoxide production elevates MBP and HR in SHRSsP. Time course of MBP and HR in AdN17Rac-transfected SHRSPs (A), AdCu/ZnSOD-transfected SHRSPs (B), and AdLacZ-transfected SHRSPs (C) before and after gene transfer (AdN17Rac1-transfected SHRSP, n=5; AdCu/ZnSOD-transfected SHRSP, n=6; AdLacZ-transfected SHRSP, n=6; *$P<0.05$ vs before gene transfer).

ity in the NTS of SHRSPs compared with the NTS of WKYs (3.0±0.1 versus 2.5±0.2 U/mg; $P<0.05$; n=5 for each; Figure 6B). The human Cu/Zn-SOD gene, which we used in the present study, produces a ≈19-kDa isoform of human Cu/Zn-SOD protein.[21] The NTS tissues from AdCu/ZnSOD-transfected SHRSPs on day 7 after transfection had a clear band representing human Cu/Zn-SOD. Human HeLa cells served as a positive control. The bands representing the expression of endogenous Cu/Zn-SOD at≈17 kDa were identical to those in AdCu/ZnSOD-transfected SHRSPs. AdLacZ-transfected SHRSPs did not produce human protein. We examined 5 individual AdCu/ZnSOD-transfected SHRSPs, and representative images are shown in Figure 6C. The increased Cu/Zn-SOD activity in the NTS of AdCu/ZnSOD-

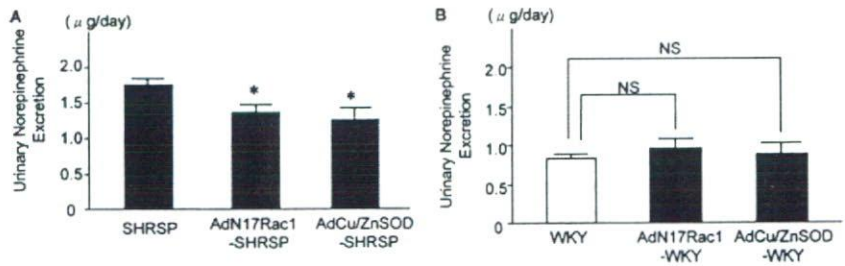

Figure 4. Rac1-dependent superoxide production elevates urinary norepinephrine excretion in SHRSPs but not in WKYs. A, 24-hour urinary norepinephrine excretion as an indicator of sympathetic nerve activity. Urinary norepinephrine excretion on day 7 after gene transfer was significantly decreased in AdN17rac1-transfected SHRSPs and AdCu/ZnSOD-transfected SHRSPs (SHRSP=1.7±0.1 μg per day; AdN17Rac1-treated SHRSP=1.4±0.1 μg per day; AdCu/ZnSOD-transfected SHRSP=1.2±0.2 μg per day; n=6 for each; *$P<0.05$ vs SHRSP). B, 24-hour urinary norepinephrine excretion in WKY rats. We did not detect any changes among WKY rats, AdN17Rac1-transfected WKY rats, and AdCu/ZnSOD-transfected WKY rats (WKY rats=0.8±0.1 μg per day; AdN17Rac1-transfected WKY rats=1.0±0.1 μg per day; AdCu/ZnSOD-transfected WKY rats=0.9±0.2 μg per day; n=6 for each).

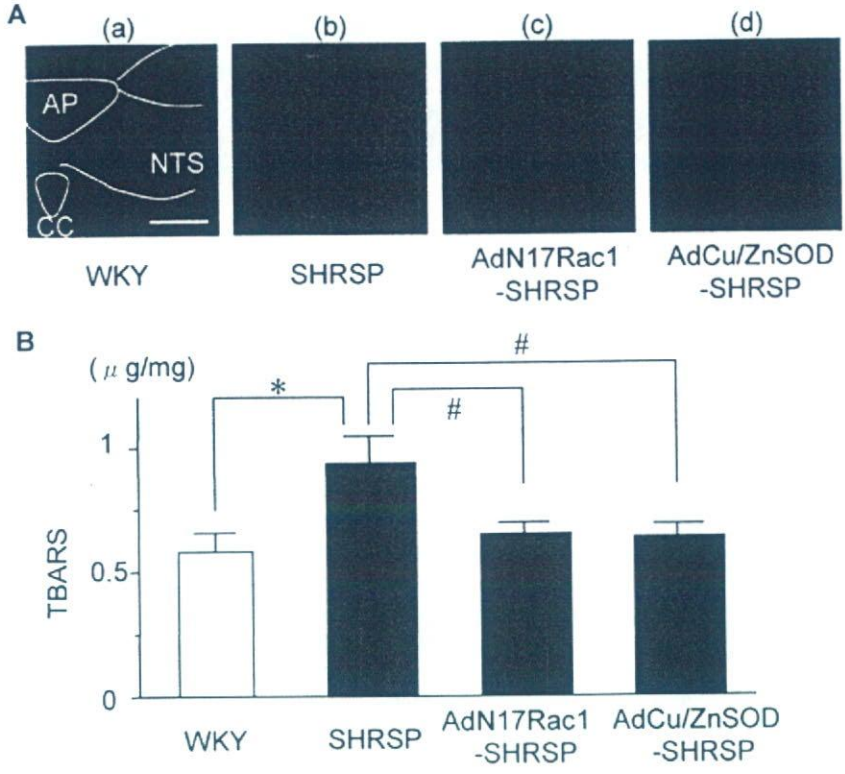

Figure 5. Rac1-dependent superoxide production is elevated in the NTS of SHRSPs and increases TBARS. A, Images of DHE-treated brain sections. We examined 4 groups (WKY, SHRSP, AdN17Rac1-transfected SHRSP, and AdCu/ZnSOD-transfected SHRSP; n=5 for each), and the figure shows representative images. Sections including the NTS of SHRSPs showed a significant increase in DHE fluorescence compared with the WKY sections. Furthermore, DHE fluorescence in the NTS was significantly attenuated in both AdN17Rac1-transfected SHRSPs and AdCu/ZnSOD-transfected SHRSPs on day 7 after gene transfer (AP indicates area postrema; CC, central canal; bar=1.0 mm). B, Lipid peroxidation as indicated by TBARS levels in the NTS. TBARS levels in the NTS of SHRSPs were significantly increased compared with WKYs. Gene transfer of either dominant-negative Rac1 or human Cu/Zn-SOD suppressed TBARS levels in the NTS (WKY=0.58±0.08 μg/g of protein; SHRSP=0.93±0.10 μg/g of protein; AdN17Rac1-transfected SHRSP=0.64±0.05 μg/g of protein; AdCu/ZnSOD-transfected SHRSP=0.63±0.05 μg/g of protein; n=5 for each; *$P<0.05$ vs WKY; #$P<0.05$ vs SHRSP).

transfected SHRSPs (2.5±0.2 versus 3.5±0.4 U/mg; $P<0.05$; n=5 for each; Figure 6D) indicated that human Cu/Zn-SOD was bioactive in rat tissues in vivo.

Discussion

The major findings of the present study are that inhibition of Rac1 expression in the NTS decreased blood pressure, HR, and urinary norepinephrine excretion in awake SHRSPs. These effects were not observed in normotensive WKYs. Rac1 activity was increased in the NTS of SHRSPs compared with WKYs. Subsequent activation of NAD(P)H oxidase and ROS production in the NTS were also increased in SHRSPs compared with those in WKYs. These results indicate that activation of Rac1 in the NTS leads to ROS generation via NAD(P)H oxidase activation in awake SHRSPs. The present study provides the first evidence that Rac1 is activated in the NTS of SHRSPs and results in enhanced NAD(P)H oxidase activity. More importantly, the subsequent ROS generation leads to increases in blood pressure and HR via the sympathetic nervous system in awake SHRSPs.

Transfection of AdN17Rac1 into the NTS successfully decreased Rac1 activity and NAD(P)H oxidase activity in the NTS of SHRSPs. It also attenuated the subsequent ROS generation, as evaluated by the DHE staining and TBARS levels. In addition, transfection of Cu/Zn-SOD into the NTS, which scavenges ROS generation, decreased blood pressure, HR, and urinary norepinephrine excretion. Taken together, these results suggest that activation of Rac1 in the NTS leads to ROS generation via NAD(P)H oxidase activity, and this mechanism contributes to the neural mechanisms of hypertension in SHRSPs.

Recent studies demonstrated the importance of ROS generation in the NTS.[7,23] Nox2-containing NAD(P)H oxidase in the NTS is the source of the Ang II–induced ROS generation in vitro.[23] Consistent with those studies, our results indicate that the Rac1/NAD(P)H pathway is involved in neuronal activation in the NTS and further indicate that activation of this pathway and the subsequent ROS generation in the NTS occur in the NTS of SHRSPs. More importantly, we demonstrated that the inhibition of Rac1 or overexpression of Cu/Zn-SOD in the NTS decreased blood pressure and HR in SHRSPs but not in WKYs. Localized human Cu/Zn-SOD or β-galactosidase gene expression in the NTS after gene transfer was confirmed by immunohistochemical staining. Gene transfer of either AdN17Rac1 or human Cu/Zn-SOD in adjacent regions not involved in cardiovascular regulation (anteroposterior angle 10°, 2.5-mm lateral, 2.5-mm deeper, to the calamus scriptorius) did not elicit any changes in MBP or HR (data not shown). The time course of the MBP and HR changes was similar to those induced by transgene expression, as shown using Western blot analysis, and was consistent with the results of our previous studies using adenovirus-mediated gene transfer.[3,10,11] These results confirmed successful gene transfer into the NTS in the present study.

The degree of oxidative stress is determined by the balance between ROS generation and antioxidant enzymatic activity. NAD(P)H oxidase has a crucial role in generating ROS in the brain.[2] In particular, most studies have been performed using Ang II infusion models to examine the role of NAD(P)H oxidase and the subsequent ROS generation in the brain and blood vessels.[2,7,23] We used SHRSPs as a hypertensive model that resembles human essential hypertension with enhanced

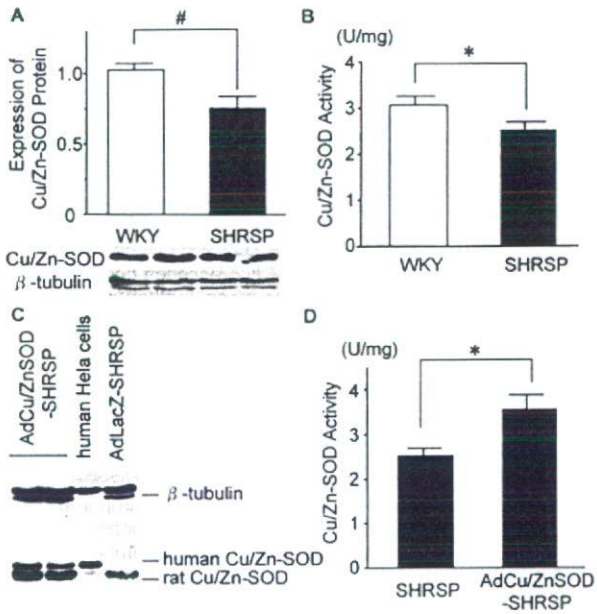

Figure 6. Cu/Zn-SOD expression and activity is reduced in SHRSPs. A, Western blot analysis of Cu/Zn-SOD protein levels in the NTS. Data are expressed as the relative ratio to control (WKYs), which were assigned a value of 1. Cu/Zn-SOD protein expression in the NTS of SHRSPs was significantly lower than that of WKYs (n=6 for each; #$P<0.01$). B, Cu/Zn-SOD activity in the NTS. Cu/Zn-SOD activity in the NTS of SHRSPs was significantly lower than that of WKYs (n=5 for each; *$P<0.05$). C, Western blot analysis of Cu/Zn-SOD on day 7 after gene transfer. The human Cu/Zn-SOD gene, which was used in the present study, produces an ≈19-kDa isoform of human Cu/Zn-SOD protein. The NTS tissues from AdCu/ZnSOD-transfected SHRSPs on day 7 after transfection had a clear band representing human Cu/Zn-SOD. Human HeLa cells served as a positive control. The bands representing the expression of endogenous Cu/Zn-SOD at ≈17 kDa were also identical in AdCu/ZnSOD-transfected SHRSPs. AdLacZ-transfected SHRSPs did not produce human Cu/Zn-SOD protein. We examined 5 individual AdCu/ZnSOD-transfected SHRSPs, and the figure shows representative images. D, Cu/Zn-SOD activity in the NTS of AdCu/ZnSOD-transfected SHRSPs was significantly higher than that of nontransfected SHRSPs (n=5 for each; *$P<0.05$).

sympathetic nerve activity.[1,24] Interestingly, we found that Cu/Zn-SOD activity in the NTS was also decreased in SHRSPs compared with WKYs, which indicates that antioxidant enzymatic activity is attenuated in the NTS of SHRSPs. One might expect that antioxidant activity would increase to compensate for the ROS generation. We do not have a clear explanation for the decreased antioxidant activity based on the results of the present study, though we reported previously that Mn-SOD activity is decreased in the rostral ventrolateral medulla of SHRSPs compared with WKYs.[1]

Adenovirus with the cytomegalovirus promoter has relatively poor neuronal selectivity.[25,26] Therefore, we performed double immunohistochemical staining for β-galactosidase and a NeuN (Figure 2D). The transfected β-galactosidase gene was expressed in almost all cell types, including neurons. Therefore, we believe that neurons, as well as glia, in the NTS were transfected with the adenovirus gene. Because Nox2 is present in the NTS neurons,[7,23,27] it is conceivable that transfection of AdN17Rac1 inhibits the NAD(P)H oxidase activity in those neurons.

Some studies examined the role of glia in cardiovascular regulation.[26,28] Indeed, in the NTS, NADPH oxidase subunits are also present in astrocytes[27]; therefore, we cannot exclude the possibility that inhibition of Rac1/NAD(P)H oxidase in glia also decreased blood pressure in the present study. The precise role of glia in cardiovascular regulation is unknown.[29] ROS, such as NO produced by neurons, as well as glial cells, are diffusive gaseous molecules and are thereby considered to influence surrounding cells. The present study did not differentiate whether the ROS was produced by neurons or glia. Further studies using neuron-specific or glia-specific gene transfer techniques are required for this specific purpose.

We did not address the precise mechanisms by which ROS in the NTS alter blood pressure via the sympathetic nervous system. Extensive evidence supports the idea that Ang II signaling mediates ROS generation,[2,5,30] and the NTS contains a high density of Ang II subtype 1 receptors located on both vagal and carotid sinus afferent terminals presynaptically and on neurons postsynaptically.[13,31] The role of Ang II in the NTS, however, is complicated. Depending on the dose, microinjection of Ang II into the NTS elicits an increase or decrease in blood pressure.[32–34] Although those studies were performed under anesthesia, there might be a connection between the renin–angiotensin system and ROS in the NTS.[35] Another possibility is that reduced availability of NO is involved in the mechanisms. In the NTS, an increase in NO elicits sympathoinhibition by facilitating the release of excitatory amino acids, such as L-glutamate.[10,36–39]

In the present study, HR was decreased in SHRSPs after transfection of AdNRac1 or AdCu/ZnSOD. There was also a decrease in urinary norepinephrine excretion. Therefore, we suggest that the effects of gene transfer-induced ROS inhibition are mediated by inhibition of the sympathetic nervous system. We cannot, however, exclude the possibility that vagal outflow is also modulated. We did not examine baroreflex control of HR and vagal outflow to the heart in the present study. It would be interesting to examine whether the bradycardic response induced by gene transfer is atropine sensitive. Further studies are needed to clarify these issues.

In conclusion, our findings indicate that inhibition of Rac1-derived ROS in the NTS decreases blood pressure, HR, and urinary norepinephrine excretion in awake SHRSPs. Activation of the Rac1/NAD(P)H oxidase pathway in the NTS might contribute to ROS generation and thereby enhanced sympathetic drive in SHRSPs.

Perspectives

The NTS regulates the baroreflex and chemoreflex functions and has an important role in cardiovascular regulation.[12,16] ROS in the brain are thought to contribute to the neuropathogenesis of hypertension by enhancing sympathetic nervous system activity. NAD(P)H oxidase is the source of ROS in the brain. The present study demonstrated that the inhibition of Rac1, which is a key component of NAD(P)H oxidase, decreased sympathetic nerve activity in a rat model of hypertension. These findings have broad implications for the development of therapeutics for human essential hypertension.

Acknowledgments

We thank Drs Donald D. Heistad and Beverly L. Davidson (University of Iowa Gene Transfer Vector Core, supported by National Institutes of Health Grants and the Carver Foundation) for providing the vectors.

Sources of Funding

This study was supported by Grants-in-Aid for Scientific Research from the Japan Society for the Promotion of Science (S18100006 and C17590745) and, in part, by the Health and Labor Sciences Research Grant for Comprehensive Research in Aging and Health Labor and Welfare of Japan.

Disclosures

None.

References

1. Kishi T, Hirooka Y, Kimura Y, Ito K, Shimokawa H, Takeshita A. Increased reactive oxygen species in rostral ventrolateral medulla contribute to neural mechanisms of hypertension in stroke-prone spontaneously hypertensive rats. *Circulation*. 2004;109:2357–2362.
2. Zimmerman MC, Dunlay RP, Lazartigues E, Zhang Y, Sharma RV, Engelhardt JF, Davisson RL. Requirement for Rac1-dependent NADPH oxidase in the cardiovascular and dipsogenic actions of angiotensin II in the brain. *Circ Res*. 2004;95:532–539.
3. Kimura Y, Hirooka Y, Sagara Y, Ito K, Kishi T, Shimokawa H, Takeshita A, Sunagawa K. Overexpression of inducible nitric oxide synthase in rostral ventrolateral medulla causes hypertension and sympathoexcitation via an increase in oxidative stress. *Circ Res*. 2005;96:252–260.
4. Lindley TE, Doobay MF, Sharma RV, Davisson RL. Superoxide is involved in the central nervous system activation and sympathoexcitation of myocardial infarction-induced heart failure. *Circ Res*. 2004;94:402–409.
5. Gao L, Wang W, Li YL, Schultz HD, Liu D, Cornish KG, Zucker IH. Superoxide mediates sympathoexcitation in heart failure: roles of angiotensin II and NAD(P)H oxidase. *Circ Res*. 2004;95:937–944.
6. Cai H, Harrison DG. Endothelial dysfunction in cardiovascular diseases: the role of oxidant stress. *Circ Res*. 2000;87:840–844.
7. Wang G, Anrather J, Huang J, Speth RC, Pickel VM, Iadecola C. NADPH oxidase contributes to angiotensin II signaling in the nucleus tractus solitarius. *J Neurosci*. 2004;24:5516–5524.
8. Vecchione C, Aretini A, Marino G, Bettarini U, Poulet R, Maffei A, Sbroggio M, Pastore L, Gentile MT, Notte A, Iorio L, Hirsch E, Tarone G, Lembo G. Selective Rac-1 inhibition protects from diabetes-induced vascular injury. *Circ Res*. 2006;98:218–225.
9. Abo A, Pick E, Hall A, Totty N, Teahan CG, Segal AW. Activation of the NADPH oxidase involves the small GTP-binding protein p21rac1. *Nature*. 1991;353:668–670.
10. Sakai K, Hirooka Y, Matsuo I, Eshima K, Shigematsu H, Shimokawa H, Takeshita A. Overexpression of eNOS in NTS causes hypotension and bradycardia in vivo. *Hypertension*. 2000;36:1023–1028.
11. Ito K, Hirooka Y, Sakai K, Kishi T, Kaibuchi K, Shimokawa H, Takeshita A. Rho/Rho-kinase pathway in brain stem contributes to blood pressure regulation via sympathetic nervous system: possible involvement in neural mechanisms of hypertension. *Circ Res*. 2003;92:1337–1343.
12. Weston M, Wang H, Stornetta RL, Sevigny CP, Guyenet PG. Fos expression by glutamatergic neurons of the solitary tract nucleus after phenylephrine-induced hypertension in rats. *J Comp Neurol*. 2003;460:525–541.
13. Healy DP, Rettig R, Nguyen T, Printz MP. Quantitative autoradiography of angiotensin II receptors in the rat solitary-vagal area: effects of nodose ganglionectomy or sinoaortic denervation. *Brain Res*. 1989;484:1–12.
14. Gutkind JS, Kurihara M, Castren E, Saavedra JM. Increased concentration of angiotensin II binding sites in selected brain areas of spontaneously hypertensive rats. *J Hypertens*. 1988;6:79–84.
15. Sato AM, Vanderlei Menani J, Ubriaco Lopes O, Colombari E. Lesions of the commissural nucleus of the solitary tract reduce arterial pressure in spontaneously hypertensive rats. *Hypertension*. 2001;38:560–564.
16. Wong LF, Polson JW, Murphy D, Paton JF, Kasparov S. Genetic and pharmacological dissection of pathways involved in the angiotensin II-mediated depression of baroreflex function. *FASEB J*. 2002;16:1595–1601.
17. Loewy AD, McKellar S. The neuroanatomical basis of central cardiovascular control. *Fed Proc*. 1980;39:2495–2503.
18. Tanaka M, Umemoto S, Kawahara S, Kubo M, Itoh S, Umeji K, Matsuzaki M. Angiotensin II type 1 receptor antagonist and angiotensin-converting enzyme inhibitor altered the activation of Cu/Zn-containing superoxide dismutase in the heart of stroke-prone spontaneously hypertensive rats. *Hypertens Res*. 2005;28:67–77.
19. Miller FJ Jr, Griendling KK. Functional evaluation of nonphagocytic NAD(P)H oxidases. *Methods Enzymol*. 2002;353:220–233.
20. Zwacka RM, Dudus L, Epperly MW, Greenberger JS, Engelhardt JF. Redox gene therapy protects human IB-3 lung epithelial cells against ionizing radiation-induced apoptosis. *Hum Gene Ther*. 1998;9:1381–1386.
21. Lehmann TG, Wheeler MD, Schwabe RF, Connor HD, Schoonhoven R, Bunzendahl H, Brenner DA, Jude Samulski R, Zhong Z, Thurman RG. Gene delivery of Cu/Zn-superoxide dismutase improves graft function after transplantation of fatty livers in the rat. *Hepatology*. 2000;32:1255–1264.
22. Korzhevskii DE, Gilerovich EG, Zin'kova NN, Grigor'ev IP, Otellin VA. Immunocytochemical detection of brain neurons using the selective marker NeuN. *Neurosci Behav Physiol*. 2006;36:857–859.
23. Wang G, Anrather J, Glass MJ, Tarsitano MJ, Zhou P, Frys KA, Pickel VM, Iadecola C. Nox2, Ca^{2+}, and protein kinase C play a role in angiotensin II-induced free radical production in nucleus tractus solitarius. *Hypertension*. 2006;48:482–489.
24. Kishi T, Hirooka Y, Ito K, Sakai K, Shimokawa H, Takeshita A. Cardiovascular effects of overexpression of endothelial nitric oxide synthase in the rostral ventrolateral medulla in stroke-prone spontaneously hypertensive rats. *Hypertension*. 2002;39:264–268.
25. Li HW, Gao YX, Matsuura T, Martynyuk A, Raizada MK, Sumners C. Adenoviral-mediated neuron specific transduction of angiotensin II type 2 receptors. *Regul Pept*. 2005;126:213–222.
26. Allen AM, Dosanjh J, Dassanayake S, Tan G, Thomas WG. Baroreceptor reflex stimulation does not induce cytomegalovirus promoter-driven transgene expression in the ventrolateral medulla in vivo. *Auton Neurosci*. 2006;126–127:150–155.
27. Glass MJ, Huang J, Oselkin M, Tarsitano MJ, Wang G, Iadecola C, Pickel VM. Subcellular localization of nicotinamide adenine dinucleotide phosphate oxidase subunits in neurons and astroglia of the rat medial nucleus tractus solitarius: relationship with tyrosine hydroxylase immunoreactive neurons. *Neuroscience*. 2006;143:547–564.
28. Sakai K, Chapleau MW, Morimoto S, Cassell MD, Sigmund CD. Differential modulation of baroreflex control of heart rate by neuron- vs. glia-derived angiotensin II. *Physiol Genomics*. 2004;20:66–72.
29. Dampney RA. Angiotensin type 1A receptors on glial cells in rostral ventrolateral medulla and hypertension. *Hypertension*. 2006;47:1052–1053.
30. Zimmerman MC, Lazartigues E, Sharma RV, Davisson RL. Hypertension caused by angiotensin II infusion involves increased superoxide production in the central nervous system. *Circ Res*. 2004;95:210–216.
31. Gehlert DR, Gackenheimer SL, Schober DA. Autoradiographic localization of subtypes of angiotensin II antagonist binding in the rat brain. *Neuroscience*. 1991;44:501–514.
32. Diz DI, Barnes KL, Ferrario CM. Hypotensive actions of microinjections of angiotensin II into the dorsal motor nucleus of the vagus. *J Hypertens*. 1984;2(suppl):S53–S56.
33. Fow JE, Averill DB, Barnes KL. Mechanisms of angiotensin-induced hypotension and bradycardia in the medial solitary tract nucleus. *Am J Physiol*. 1994;267:H259–H266.
34. Rettig R, Healy DP, Printz MP. Cardiovascular effects of microinjections of angiotensin II into the nucleus tractus solitarii. *Brain Res*. 1986;364:233–240.
35. Chen Y, Chen H, Hoffmann A, Cool DR, Diz DI, Chappell MC, Chen AF, Morris M. Adenovirus-mediated small-interference RNA for in vivo silencing of angiotensin AT1a receptors in mouse brain. *Hypertension*. 2006;47:230–237.
36. Zanzinger J. Role of nitric oxide in the neural control of cardiovascular function. *Cardiovasc Res*. 1999;43:639–649.
37. Dias AC, Vitela M, Colombari E, Mifflin SW. Nitric oxide modulation of glutamatergic, baroreflex, and cardiopulmonary transmission in the nucleus of the solitary tract. *Am J Physiol Heart Circ Physiol*. 2005;288:H256–H262.
38. Hirooka Y, Sakai K, Kishi T, Ito K, Shimokawa H, Takeshita A. Enhanced depressor response to endothelial nitric oxide synthase gene transfer into the nucleus tractus solitarii of spontaneously hypertensive rats. *Hypertens Res*. 2003;26:325–331.
39. Matsuo I, Hirooka Y, Hironaga K, Eshima K, Shigematsu H, Shihara M, Sakai K, Takeshita A. Glutamate release via NO production evoked by NMDA in the NTS enhances hypotension and bradycardia in vivo. *Am J Physiol Regul Integr Comp Physiol*. 2001;280:R1285–R1291.

Local Delivery of Anti-Monocyte Chemoattractant Protein-1 by Gene-Eluting Stents Attenuates In-Stent Stenosis in Rabbits and Monkeys

Kensuke Egashira, Kaku Nakano, Kisho Ohtani, Kouta Funakoshi, Gang Zhao, Yoshiko Ihara, Jun-ichiro Koga, Satoshi Kimura, Ryuji Tominaga, Kenji Sunagawa

Objective—We have previously shown that the intramuscular transfer of the anti–monocyte chemoattractant protein-1 (MCP-1) gene (called 7ND) is able to prevent experimental restenosis. The aim of this study was to determine the in vivo efficacy and safety of local delivery of 7ND gene via the gene-eluting stent in reducing in-stent neointima formation in rabbits and in cynomolgus monkeys.

Methods and Results—We here found that in vitro, 7ND effectively inhibited the chemotaxis of mononuclear leukocytes and also inhibited the proliferation/migration of vascular smooth muscle cells. We then coated stents with a biocompatible polymer containing a plasmid bearing the 7ND gene, and deployed these stents in the iliac arteries of rabbits and monkeys. 7ND gene-eluting stents attenuated stent-associated monocyte infiltration and neointima formation after one month in rabbits, and showed long-term inhibitory effects on neointima formation when assessments were carried out at 1, 3, and 6 months in monkeys.

Conclusions—Strategy of inhibiting the action of MCP-1 with a 7ND gene-eluting stent reduced in-stent neointima formation with no evidence of adverse effects in rabbits and monkeys. The 7ND gene-eluting stent could be a promising therapy for treatment of restenosis in humans. **(*Arterioscler Thromb Vasc Biol*. 2007;27:2563-2568.)**

Key Words: restenosis ■ inflammation ■ leukocytes ■ stents ■ smooth muscle cells

The use of polymer-coated drug-eluting stents (DES) for local drug delivery has proved to be a useful strategy for the prevention of restenosis.[1–3] However, recent clinical reports raise the possibility of a risk of stent thrombosis in DES compared with bare metal stent.[4–6] Drugs released from first-generation DES (sirolimus or paclitaxel) exert distinct biological effects[3,4]: although primarily aimed to prevent vascular smooth muscle cell (VSMC) proliferation, which is one of central factors in the pathogenesis of restenosis, they also impair reendothelialization, which leads to delayed arterial healing and thrombogenesis. The use of sirolimus-eluting stents in a porcine model was associated with no apparent long-term effects and with the delayed inflammation and proliferation.[7,8] In human pathologic study with 40 patients who died after the currently-approved DES implantation, it was suggested that the DES caused a persistent fibrin deposition and delayed reendothelialization compared with bare metal stent implantation.[9] Therefore, the development of a novel DES system with less adverse effects is needed.

We have recently devised a new gene therapy strategy for the delivery of the anti–monocyte chemoattractant protein-1 (MCP-1) in which plasmid cDNA encoding a mutant MCP-1 gene is transfected into skeletal muscle.[10] This mutant MCP-1 protein, called 7ND, lacks the N-terminal amino acids 2 through 8 and has been shown to function as a dominant-negative inhibitor of MCP-1. Using this systemic gene transfer strategy, we have demonstrated that blocking MCP-1–derived signals reduced neointima formation after balloon- and stent-induced injury[11–14] and atherosclerosis[15,16] in animals, including nonhuman primates. Overall, these data suggest that an antiinflammatory strategy targeting MCP-1 may be an appropriate and reasonable approach for the prevention of restenosis.

Local delivery of 7ND through a gene-eluting stent may have advantages beyond those of the current first-generation DES devices: 7ND does not affect endothelial regeneration and proliferation[11] and may also inhibit proliferation of VSMC.[17,18] Previous studies have reported that stents coated with a polymer emulsion containing plasmid DNA were able to effect successful transgene delivery and expression in arteries.[19–21] In this study, we examined the possibility that a 7ND gene-eluting stent might reduce in-stent neointima

Original received December 24, 2006; final version accepted September 12, 2007.

From the Department of Cardiovascular Medicine (K.E., K.N., K.O., K.F., Y.I., J.K., K.S.) and Surgery (S.K., R.T.), Graduate School of Medical Sciences, Kyushu University, Fukuoka, Japan; and the Department of Cardiovascular Medicine (G.Z.), Shanghai Sixth People's Hospital, Shanghai Jiao Tong University Affiliated Sixth People's Hospital, Shanghai, China.

K.E., K.N., and K.O. contributed equally to this study.

Correspondence to Kensuke Egashira, MD, PhD, Department of Cardiovascular Medicine, Graduate School of Medical Science, Kyushu University, 3-1-1, Maidashi, Higashi-ku, Fukuoka 812-8582, Japan. E-mail egashira@cardiol.med.kyushu-u.ac.jp

Arterioscler Thromb Vasc Biol **is available at http://atvb.ahajournals.org** **DOI: 10.1161/ATVBAHA.107.154609**

formation. To assess its potential clinical utility, we used a nonhuman primate model of stent-associated neointima formation.[11] The specific aims of this study were (1) to use biocompatible polymer technology to create a 7ND gene-eluting metallic stent; (2) to determine whether the 7ND gene-eluting stent was able to reduce in-stent inflammation and neointima formation, and to assess any potential adverse effects in vivo; and (3) to determine the effects of the 7ND protein on the chemotaxis of mononuclear leukocytes and on the proliferation of VSMCs in vitro.

Materials and Methods

Plasmid Expression Vectors

This section is available in the supplemental materials (available online at http://atvb.ahajournals.org).

Stent Preparation and Measurement of In Vitro DNA Release Kinetics

A 15-mm-long stainless-steel balloon-expandable stent was dip-coated under sterile conditions with multiple thin layers of biocompatible polymer (polyvinyl alcohol [PVOH], GOHSENOL EG-05, Nippon Gohsei Inc) The polymer solution additionally contained either the 7ND cDNA plasmid, the GFP plasmid, or the β-galactosidase plasmid; polymer containing no added plasmid was also included as a control. The coated stent was then mounted over a 3-mm balloon catheter; a noncoated stent mounted over the same balloon catheter was used as a control. To measure DNA release kinetics in vitro, the 7ND plasmid-coated stents (n=8) were immersed in Tris-EDTA buffer, and the plasmid that was subsequently eluted into the buffer was measured using a thiazole fluorescence assay. Additional details are in the online data supplement.

Stent Implantation and Analysis in the Rabbit Model

The animal model experiments were reviewed and approved by the Committee on Ethics on Animal Experiments, Kyushu University Faculty of Medicine, and were performed according to the guidelines of the National Institutes of Health (NIH) Guide for the Care and Use of Laboratory Animals.

Male Japanese white rabbits (KBT Oriental, Tokyo, Japan) weighing 3.0 to 3.5 kg were fed a high-cholesterol diet containing 1% cholesterol and 3% peanut oil for 2 weeks before stent implantation. Animals were anesthetized and were randomly divided into 2 groups, which underwent deployment of either a noncoated bare metal stent (n=14) or a 7ND gene-eluting stent (n=14) in the right femoral artery as described previously.[11] All animals received aspirin at 20 mg/d until euthanasia from 3 days before stent implantation procedure. After venous blood samples were taken, animals were euthanized with a lethal dose of anesthesia at days 10 (n=7 each) and 28 (n=7 each), and the stented arterial sites and contralateral nonstented sites were excised for biochemical, immunohistochemical, and morphometric analyses. In addition, the plasma levels of total cholesterol levels were determined with commercially available kits (Wako Pure Chemicals).

The stented artery segments were processed as described previously.[11] Additional details are in the online data supplement.

Stent Implantation and Analysis in the Monkey Model

This section is available online.

Purification of the 7ND Protein

This section is available online.

Protein Expression of the MCP-1 Receptor (CCR2)

This section is available online.

Leukocyte Chemotaxis Assay

This section is available online.

Proliferation Assay in Vascular Smooth Muscle Cells

This section is available online.

Angiogenic Activity of Endothelial Cells

This section is available online.

Agarose Gel Electrophoresis and Cell Transfection Studies

This section is available online.

Statistical Analysis

Data are expressed as means±SE. The statistical analysis of differences between 2 groups was assessed with the unpaired *t* test, and the statistical analysis of differences among 3 groups was assessed by using ANOVA and Bonferroni multiple comparison tests. Probability values <0.05 were considered to be statistically significant.

Results

Kinetics of DNA Release and Expression of Plasmid DNA

Scanning electron microscopy analysis revealed that polymer coating formed a uniform film over the outer surface of the stent (supplemental Figure IA). After balloon expansion, the polymer stretched, but no fragmentation was observed. An analysis of the plasmid DNA release kinetics in vitro showed an early burst of release, such that ≈80% of the total amount released was present 1 day after implantation, and maximal release occurred by 3 days after implantation (supplemental Figure IB). Analysis of the DNA eluted from the stent by agarose gel electrophoresis showed that the DNA was structurally intact, and the functionality of the eluted DNA was confirmed by the ability of an eluted GFP plasmid to successfully be transfected and expressed in THP-1 cells and human coronary artery VSMC (hCASMC; supplemental Figure II).

Before examining the stent-based administration a plasmid encoding the 7ND protein, we first tested the stent-based delivery of the bacterial lacZ gene, which encodes the easily detectable protein β-galactosidase. Three days after stent implantation in the rabbit iliac artery, we saw expression of β-galactosidase at the gene-eluting stent site, but not at the site of implantation of a bare, non-coated metal stent, which was used as a negative control (Figure 1). X-gal staining of cross-sections was used to detect the expressed protein, and revealed that staining for β-galactosidase was localized mostly in the intima and on the luminal side of the media, and was present at a lesser extent in the adventitia. No induction of protein β-galactosidase was observed 7 days after stent implantation.

Effects of 7ND on Neointima Formation in Rabbit and Monkey Animal Models

The infiltration of RAM-11–positive macrophages around the stent strut for the non-coated control stent was observed at 10 days after stent implantation (Figure 2); this was consistent with our previous results.[11,22] In contrast, the 7ND gene-eluting stents reduced the severity of macrophage-induced inflammation (Figure 2). Although an in-stent neointima formed similarly in the non-coated stent and 7ND gene-

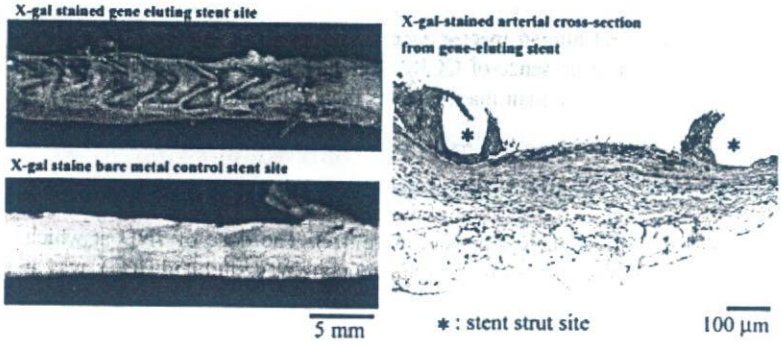

Figure 1. Gene transfer in the rabbit iliac stented artery 3 days after β-galactosidase gene-eluting stent. Upper and lower left: Macroscopic image of the luminal surface of the stented iliac artery. Stented arterial segments were excised, cut longitudinally, and stained with X-gal. Right: X-gal-stained arterial cross-sections.

eluting stent (histopathologic pictures in supplemental Figure IVA), quantitative analysis demonstrated a significant reduction in neointima formation in the 7ND gene-eluting stent site compared with the noncoated control stent sites (Figure 3A). However, there were no significant differences in stent area, IEL area, or medial area between rabbits receiving either the noncoated stent or the 7ND-eluting stent.

We also examined the effect of 7ND gene-eluting stents on inflammation and neointima in a monkey model. At sites in which a noncoated stent was implanted, an in-stent neointima was present at 1, 3, and 6 months after stenting (histopathologic pictures in supplemental Figure IVB). Quantitative analysis revealed that there was a significant reduction in neointima formation at sites in which the 7ND gene-eluting stent had been implanted compared with the noncoated control stent sites (Figure 3B). There were no significant differences in stent area, IEL area, or medial area between the 2 groups.

Histological and Biochemical Analysis

Biochemical analysis showed that after stenting, serum concentrations of MCP-1 increased transiently after deployment of bare metal and 7ND gene-eluting stents in monkeys. There was no significant differences in MCP-1 levels between the 2 groups (supplemental Figure V).

A histological analysis showed that there was no significant difference in the injury score or the inflammation score between the two groups of rabbits (supplemental Tables I and II) or monkeys (supplemental Table III). The endothelial cell linings, as monitored by CD31 immunoreactivity, were present at an approximately equal extent in the 2 groups (supplemental Tables II and III).

Delivery of 7ND gene-eluting stents did not have any significant effect on serum cholesterol levels, as serum cholesterol was similar in animals receiving the noncoated stent or the 7ND-coated stent; this was true both in rabbits (data not shown) and in monkeys (supplemental Table IV).

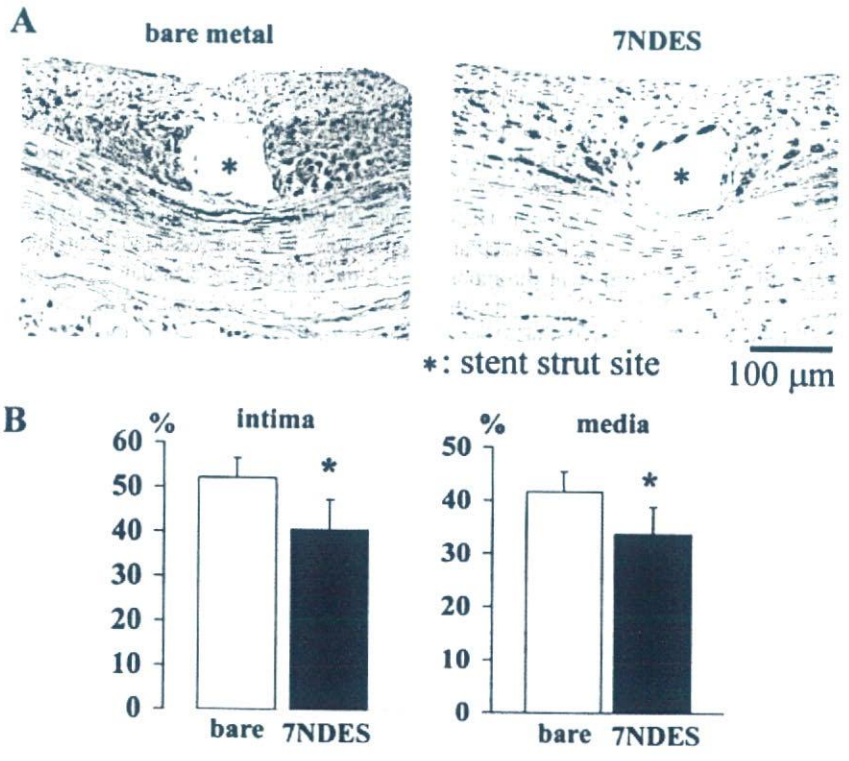

Figure 2. Effect of 7ND gene-eluting stents (7NDES) on local inflammation in rabbits. A, Inflammation (RAM-11–positive monocytes/macrophages) 10 days after stenting. B, Summary of quantitative analysis, as reported by the percentage of immunopositive cells per total cells; n=7 each. *$P<0.01$ vs the noncoated stents.

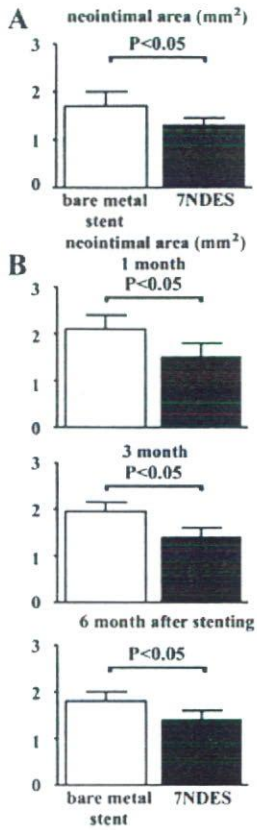

Figure 3. Inhibitory effect of 7ND gene-eluting stents (7NDES) on in-stent neointima formation in rabbits (A) and monkeys (B). A, Neointimal area 28 days after stenting (n=7 each). B, Neointima area at 1, 3, and 6 months (M) after stenting (n=6 each).

We additionally measured body weight, serum biochemical markers, and blood cell count in monkeys (supplemental Tables IV, V, and VI) and found no systemic adverse effects resulting from 7ND administration or significant treatment-associated differences in body weight between the 2 groups.

The Presence of CCR2 Protein on Human Coronary Arterial Smooth Muscle Cells

To validate our method for CCR2 detection, Western blot analysis was performed in peritoneal macrophages as control. Protein expression of CCR2 was actually detected in peritoneal macrophages isolated from wild-type mice. In contrast, no signal was detected in CCR2-knockout mice (supplemental Figure IIA). Immunoblot was then performed in hCASMC and human macrophages (THP-1) using the same antibody. The presence of CCR2 was detectable in hCASMCs as well as in human macrophages (supplemental Figure IIB).

Effect of the 7ND Protein in Cultured Vascular Cells

The 7ND protein inhibited the MCP-1-induced chemotaxis of mononuclear cells (Figure 4A). The dose of 7ND at which 50% of the observed chemotaxis was inhibited (IC_{50}), was at a ratio of 1:10 relative to the concentration of the MCP-1. This inhibition was specific for MCP-1, as 7ND had no effect on the interleukin (IL)-8–induced chemotaxis of polymorphic nuclear leukocytes. 7ND inhibited the MCP-1–induced proliferation of hCASMCs (Figure 4B).

To examine the effects of 7ND on endothelial proliferation, we examined whether 7ND had any effect on the known capacity of VEGF to increase the capillary density of CD31-positive endothelial cells,[23] and found that 7ND had no apparent effect on VEGF-induced angiogenic activity (Figure 4C).

Discussion

In this study we found that implantation of a 7ND gene-eluting stent reduced in-stent neointima formation with no evidence of adverse effects in rabbits or in nonhuman primates (cynomolgus monkeys). Although there is currently no clear consensus regarding which animal model (rabbit, dog, pig, monkey, etc.) is most appropriate for the evaluation of in-stent restenosis,[24] nonhuman primate models may have advantages over nonprimate animal models, because the results of efficacy and safety tests performed in such nonhuman primates can be applied to humans. Therefore, the use of nonhuman primates may allow for the evaluation of the efficacy and safety of therapies under conditions that more closely approximate those of the human physiology. The results presented here support the notion that that MCP-1 plays a central role in the pathogenesis of in-stent neointima formation (in-stent restenosis), and also provide evidence for feasibility of using the 7ND gene-eluting stent for prevention of in-stent restenosis in a human interventional setting.

Although DES reduces the rate of restenosis and target-vessel revascularization below 10%, increased risk of late in-stent thrombosis resulting in acute myocardial infarction and death after the use of the first-generation DES devices is becoming a big problem.[4–6] Silorimus and paclitaxel have

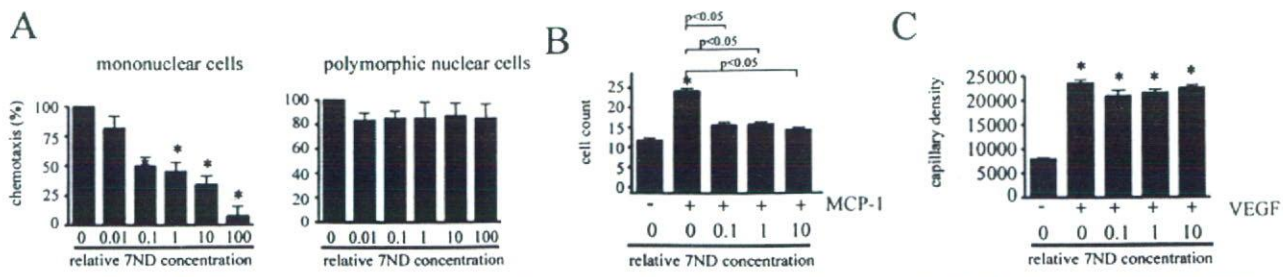

Figure 4. Effect of 7ND on chemotaxis of mononuclear leukocytes (A, n=8 each), proliferation of hCASMCs (B, n=8 each), and angiogenic activity of endothelial cells (C, n=8 each). Concentrations of 7ND are expressed in relation to concentrations of the agonist. *$P<0.05$ vs control.

been shown to impair reendothelialization and arterial healing process, resulting thrombogenesis attributable to increased expression of tissue factor.[4] In addition, nonbiocompatible polymers used to load these drugs have been associated with DES thrombosis.[25] However, no such adverse reactions were noted in this study especially in monkeys even after cessation of ticlopidine. In addition, 7ND showed no effect on proliferation of human endothelial cells in vitro. This suggests that the 7ND gene transfer does not appear to impair the healing process of endothelial cells in a stented arterial wall, so in these respects, this approach may have an advantage over the first-generation DES devices. We have shown that the biocompatible polymer and plasmid DNA coating material used in this study did not appear to cause any adverse reactions during a 1-month observation period in rabbits and during a 6-month observation period in monkeys. Therefore, we suggest that the blockade of MCP-1 via the 7ND gene-eluting stent may become a promising therapeutic strategy for treatment of restenosis, and that this strategy may have a low level of potential adverse effects.

From a perspective of clinical applicability, it is important to take into account any potential systemic toxicity associated with stent-based delivery of 7ND DNA plasmid. We demonstrated that 7ND gene-eluting stent, which elutes plasmid DNA at a dose of ≈0.8 mg/ body [≈0.23 mg/kg in rabbits (BW=about 3.5 kg) and ≈0.16 mg/kg in monkeys (BW=about 5 kg)], did not induce any significant inflammatory or immune reactions. We have previously reported that the systemic intramuscular transfer of plasmid cDNA encoding the 7ND gene at doses ranging from 0.5 to 10 mg/kg was nontoxic and safe in nonhuman primates,[12,14,26] rabbits,[11] rats,[14] and mice.[12] In addition, knockout mice lacking MCP-1[27] or the MCP-1 receptor (C-C chemokine receptor 2: CCR2)[28] displayed no serious health problems, suggesting that inhibition of MCP-1 is not physiologically toxic. From a toxicological point of view, because the dose of 7ND plasmid eluted from stents would be even lower in human subject (≈0.01 mg/kg for patients weighing 80 kg), it would be unlikely that the 7ND gene-eluting stent would cause any toxicity in humans. In clinical trials of plasmid DNA-based gene therapy in which DNA was administered into the lower limb,[29] myocardium,[30] or coronary artery[31,32] at 2 to 4 mg/ body, no systemic adverse effects were reported. Overall, these safety and feasibility data support the notion that stent-based gene therapy could safely be applied to human subjects.

We have previously reported that 7ND gene transfer not only suppressed inflammation (monocyte infiltration), but also reduced the number of proliferating SMCs in the neointima after injury.[11,13,14] Therefore, besides monocyte-mediated inflammation, we hypothesized that 7ND inhibits MCP-1–induced proliferation of SMCs. This notion is in line with several recent reports[17,18,33] demonstrating that (1) mRNA and protein for the receptor for MCP-1, CCR2, are detectable in vascular SMCs; and (2) MCP-1 induces SMC proliferation in vitro. However, the effects of MCP-1 and CCR2 on SMC proliferation are controversial: several studies reported that MCP-1 either has no effect[34] or inhibits proliferation.[35] These conflicting conclusions are discussed to result from species specificity for MCP-1 activity in an article[17] where human MCP-1 was used to proliferate human SMCs. Furthermore, MCP-1 induces tissue factor in murine SMCs from $CCR^{-/-}$ mice,[36] suggesting the possible presence of alternate MCP-1 receptor in murine SMCs. Therefore, we used human MCP-1 to stimulate hCASMCs in culture, and found that in addition to potent inhibitory actions on monocyte chemotaxis, 7ND inhibited proliferation of hCASMCs induced by human MCP-1. The presence of the receptor for MCP-1, CCR2, on the hCASMCs was also established. Therefore, our present data suggest that 7ND directly inhibits human SMC proliferation, in addition to its known effects on monocytes present in the in-stent vascular lesion.

In conclusion, strategy of inhibiting the action of MCP-1 with a 7ND gene-eluting stent reduced in-stent neointima formation with no evidence of either systemic or local adverse effects in rabbits and monkeys. These data suggest that anti–MCP-1 gene therapy via 7ND gene-eluting stents may be a clinically relevant and feasible therapeutic strategy for the treatment of in-stent restenosis. Further clinical trials are needed to examine this possibility.

Sources of Funding

This study was supported by Grants-in-Aid for Scientific Research (14657172, 14207036, etc) from the Ministry of Education, Science, and Culture, Tokyo, Japan, by Health Science Research Grants (Research on Translational Research and Nanomedicine) from the Ministry of Health Labor and Welfare, Tokyo, Japan, and by the Program for Promotion of Fundamental Studies in Health Sciences of the Organization for Pharmaceutical Safety and Research, Tokyo, Japan.

Disclosures

Dr Egashira holds a patent on the results reported in the present study.

References

1. Babapulle MN, Eisenberg MJ. Coated stents for the prevention of restenosis: Part I. *Circulation*. 2002;106:2734–2740.
2. Babapulle MN, Eisenberg MJ. Coated stents for the prevention of restenosis: Part II. *Circulation*. 2002;106:2859–2866.
3. Serruys PW, Kutryk MJ, Ong AT. Coronary-artery stents. *N Engl J Med*. 2006;354:483–495.
4. Luscher TF, Steffel J, Eberli FR, Joner M, Nakazawa G, Tanner FC, Virmani R. Drug-eluting stent and coronary thrombosis: biological mechanisms and clinical implications. *Circulation*. 2007;115:1051–1058.
5. Curfman GD, Morrissey S, Jarcho JA, Drazen JM. Drug-eluting coronary stents–promise and uncertainty. *N Engl J Med*. 2007;356:1059–1060.
6. Farb A, Boam AB. Stent thrombosis redux–the FDA perspective. *N Engl J Med*. 2007;356:984–987.
7. Carter AJ, Aggarwal M, Kopia GA, Tio F, Tsao PS, Kolata R, Yeung AC, Llanos G, Dooley J, Falotico R. Long-term effects of polymer-based, slow-release, sirolimus-eluting stents in a porcine coronary model. *Cardiovasc Res*. 2004;63:617–624.
8. Virmani R, Guagliumi G, Farb A, Musumeci G, Grieco N, Motta T, Mihalcsik L, Tespili M, Valsecchi O, Kolodgie FD. Localized hypersensitivity and late coronary thrombosis secondary to a sirolimus-eluting stent: should we be cautious? *Circulation*. 2004;109:701–705.
9. Joner M, Finn AV, Farb A, Mont EK, Kolodgie FD, Ladich E, Kutys R, Skorija K, Gold HK, Virmani R. Pathology of drug-eluting stents in humans: delayed healing and late thrombotic risk. *J Am Coll Cardiol*. 2006;48:193–202.
10. Egashira K, Koyanagi M, Kitamoto S, Ni W, Kataoka C, Morishita R, Kaneda Y, Akiyama C, Nishida K, Sueishi K, Takeshita A. Anti-monocyte chemoattractant protein-1 gene therapy inhibits vascular remodeling in rats: blockade of MCP-1 activity after intramuscular transfer of a mutant gene inhibits vascular remodeling induced by chronic blockade of NO systhesis. *FASEB J*. 2000;14:1974–1978.

11. Ohtani K, Usui M, Nakano K, Kohjimoto Y, Kitajima S, Hirouchi Y, Li XH, Kitamoto S, Takeshita A, Egashira K. Antimonocyte chemoattractant protein-1 gene therapy reduces experimental in-stent restenosis in hypercholesterolemic rabbits and monkeys. *Gene Ther*. 2004;11:1273–1282.
12. Egashira K, Zhao Q, Kataoka C, Ohtani K, Usui M, Charo IF, Nishida K, Inoue S, Katoh M, Ichiki T, Takeshita A. Importance of monocyte chemoattractant protein-1 pathway in neointimal hyperplasia after periarterial injury in mice and monkeys. *Circ Res*. 2002;90:1167–1172.
13. Mori E, Komori K, Yamaoka T, Tanii M, Kataoka C, Takeshita A, Usui M, Egashira K, Sugimachi K. Essential role of monocyte chemoattractant protein-1 in development of restenotic changes (neointimal hyperplasia and constrictive remodeling) after balloon angioplasty in hypercholesterolemic rabbits. *Circulation*. 2002;105:2905–2910.
14. Usui M, Egashira K, Ohtani K, Kataoka C, Ishibashi M, Hiasa K, Katoh M, Zhao Q, Kitamoto S, Takeshita A. Anti-monocyte chemoattractant protein-1 gene therapy inhibits restenotic changes (neointimal hyperplasia) after balloon injury in rats and monkeys. *Faseb J*. 2002;16:1838–1840.
15. Ni W, Egashira K, Kitamoto S, Kataoka C, Koyanagi M, Inoue S, Imaizumi K, Akiyama C, Nishida Ki K, Takeshita A. New anti-monocyte chemoattractant protein-1 gene therapy attenuates atherosclerosis in apolipoprotein E-knockout mice. *Circulation*. 2001;103:2096–2101.
16. Inoue S, Egashira K, Ni W, Kitamoto S, Usui M, Otani K, Ishibashi M, Hiasa K, Nishida K, Takeshita A. Anti-monocyte chemoattractant protein-1 gene therapy limits progression and destabilization of established atherosclerosis in apolipoprotein E-knockout mice. *Circulation*. 2002;106:2700–2706.
17. Selzman CH, Miller SA, Zimmerman MA, Gamboni-Robertson F, Harken AH, Banerjee A. Monocyte chemotactic protein-1 directly induces human vascular smooth muscle proliferation. *Am J Physiol Heart Circ Physiol*. 2002;283:H1455–H1461.
18. Schepers A, Eefting D, Bonta PI, Grimbergen JM, de Vries MR, van Weel V, de Vries CJ, Egashira K, van Bockel JH, Quax PH. Anti-MCP-1 gene therapy inhibits vascular smooth muscle cells proliferation and attenuates vein graft thickening both in vitro and in vivo. *Arterioscler Thromb Vasc Biol*. 2006;26:2063–2069.
19. Klugherz BD, Jones PL, Cui X, Chen W, Meneveau NF, DeFelice S, Connolly J, Wilensky RL, Levy RJ. Gene delivery from a DNA controlled-release stent in porcine coronary arteries. *Nat Biotechnol*. 2000;18:1181–1184.
20. Takahashi A, Palmer-Opolski M, Smith RC, Walsh K. Transgene delivery of plasmid DNA to smooth muscle cells and macrophages from a biostable polymer-coated stent. *Gene Ther*. 2003;10:1471–1478.
21. Walter DH, Cejna M, Diaz-Sandoval L, Willis S, Kirkwood L, Stratford PW, Tietz AB, Kirchmair R, Silver M, Curry C, Wecker A, Yoon YS, Heidenreich R, Hanley A, Kearney M, Tio FO, Kuenzler P, Isner JM, Losordo DW. Local gene transfer of phVEGF-2 plasmid by gene-eluting stents: an alternative strategy for inhibition of restenosis. *Circulation*. 2004;110:36–45.
22. Ohtani K, Egashira K, Nakano K, Zhao G, Funakoshi K, Ihara Y, Kimura S, Tominaga R, Morishita R, Sunagawa K. Stent-based local delivery of nuclear factor-kappaB decoy attenuates in-stent restenosis in hypercholesterolemic rabbits. *Circulation*. 2006;114:2773–2779.
23. Yamada M, Kim S, Egashira K, Takeya M, Ikeda T, Mimura O, Iwao H. Molecular mechanism and role of endothelial monocyte chemoattractant protein-1 induction by vascular endothelial growth factor. *Arterioscler Thromb Vasc Biol*. 2003;23:1996–2001.
24. Schwartz RS, Edelman ER, Carter A, Chronos N, Rogers C, Robinson KA, Waksman R, Weinberger J, Wilensky RL, Jensen DN, Zuckerman BD, Virmani R. Drug-eluting stents in preclinical studies: recommended evaluation from a consensus group. *Circulation*. 2002;106:1867–1873.
25. van der Giessen WJ, Lincoff AM, Schwartz RS, van Beusekom HM, Serruys PW, Holmes DR, Jr., Ellis SG, Topol EJ. Marked inflammatory sequelae to implantation of biodegradable and nonbiodegradable polymers in porcine coronary arteries. *Circulation*. 1996;94:1690–1697.
26. Kitamoto S, Nakano K, Hirouchi Y, Kohjimoto Y, Kitajima S, Usui M, Inoue S, Egashira K. Cholesterol-lowering independent regression and stabilization of atherosclerotic lesions by pravastatin and by antimonocyte chemoattractant protein-1 therapy in nonhuman primates. *Arterioscler Thromb Vasc Biol*. 2004;24:1522–1528.
27. Gu L, Okada Y, Clinton SK, Gerard C, Sukhova GK, Libby P, Rollins BJ. Absence of monocyte chemoattractant protein-1 reduces atherosclerosis in low density lipoprotein receptor-deficient mice. *Molecular Cell*. 1998;2:275–281.
28. Boring L, Gosling J, Cleary M, Charo IF. Decreased lesion formation in CCR2-/- mice reveals a role for chemokines in the initiation of atherosclerosis. *Nature*. 1998;394:894–897.
29. Morishita R, Aoki M, Hashiya N, Makino H, Yamasaki K, Azuma J, Sawa Y, Matsuda H, Kaneda Y, Ogihara T. Safety evaluation of clinical gene therapy using hepatocyte growth factor to treat peripheral arterial disease. *Hypertension*. 2004;44:203–209.
30. Losordo DW, Vale PR, Hendel RC, Milliken CE, Fortuin FD, Cummings N, Schatz RA, Asahara T, Isner JM, Kuntz RE. Phase 1/2 placebo-controlled, double-blind, dose-escalating trial of myocardial vascular endothelial growth factor 2 gene transfer by catheter delivery in patients with chronic myocardial ischemia. *Circulation*. 2002;105:2012–2018.
31. Laitinen M, Hartikainen J, Hiltunen MO, Eranen J, Kiviniemi M, Narvanen O, Makinen K, Manninen H, Syvanne M, Martin JF, Laakso M, Yla-Herttuala S. Catheter-mediated vascular endothelial growth factor gene transfer to human coronary arteries after angioplasty. *Hum Gene Ther*. 2000;11:263–270.
32. Hedman M, Hartikainen J, Syvanne M, Stjernvall J, Hedman A, Kivela A, Vanninen E, Mussalo H, Kauppila E, Simula S, Narvanen O, Rantala A, Peuhkurinen K, Nieminen MS, Laakso M, Yla-Herttuala S. Safety and feasibility of catheter-based local intracoronary vascular endothelial growth factor gene transfer in the prevention of postangioplasty and in-stent restenosis and in the treatment of chronic myocardial ischemia: phase II results of the Kuopio Angiogenesis Trial (KAT). *Circulation*. 2003;107:2677–2683.
33. Hayes IM, Jordan NJ, Towers S, Smith G, Paterson JR, Earnshaw JJ, Roach AG, Westwick J, Williams RJ. Human vascular smooth muscle cells express receptors for CC chemokines. *Arterioscler Thromb Vasc Biol*. 1998;18:397–403.
34. Wang JM, Sica A, Peri G, Walter S, Padura IM, Libby P, Ceska M, Lindley I, Colotta F, Mantovani A. Expression of monocyte chemotactic protein and interleukin-8 by cytokine-activated human vascular smooth muscle cells. *Arterioscler Thromb*. 1991;11:1166–1174.
35. Ikeda U, Okada K, Ishikawa S, Saito T, Kasahara T, Shimada K. Monocyte chemoattractant protein 1 inhibits growth of rat vascular smooth muscle cells. *Am J Physiol*. 1995;268:H1021–H1026.
36. Schecter AD, Berman AB, Yi L, Ma H, Daly CM, Soejima K, Rollins BJ, Charo IF, Taubman MB. MCP-1-dependent signaling in CCR2($^{-/-}$) aortic smooth muscle cells. *J Leukoc Biol*. 2004;75:1079–1085.

ELSEVIER

Atherosclerosis 196 (2008) 172–179

ATHEROSCLEROSIS

www.elsevier.com/locate/atherosclerosis

Azelnidipine has anti-atherosclerotic effects independent of its blood pressure-lowering actions in monkeys and mice

Kaku Nakano [a], Kensuke Egashira [a,*], Kisho Ohtani [a], Zhao Gang [b], Eiko Iwata [a], Miho Miyagawa [a], Kenji Sunagawa [a]

[a] *Department of Cardiovascular Medicine, Graduate School of Medical Sciences, Kyushu University, Fukuoka, Japan*
[b] *Department of Cardiovascular Medicine, Shanghai Sixth People's Hospital, Shanghai Jiao Tong University Affiliated Sixth People's Hospital, Shanghai, China*

Received 17 October 2006; received in revised form 19 March 2007; accepted 22 March 2007
Available online 3 May 2007

Abstract

Calcium channel blockers (CCBs) have been shown to improve clinical outcomes in atherosclerotic vascular disease. The mechanisms underlying the vasculoprotective effects of a third-generation calcium channel blocker, azelnidipine, are incompletely understood. We asked whether azelnidipine attenuates atherosclerosis in monkeys and mice beyond its blood pressure-lowering effects. Cynomolgus monkeys were randomized to three groups after 4 weeks of a high cholesterol diet: control group (no treatment) and 3 and 10 mg/kg daily azelnidipine; these doses have no effect on systemic arterial pressure or heart rate. Atherosclerosis was induced in the aorta by balloon injury, and the diet and treatment were continued for an additional 24 weeks. Azelnidipine did not affect blood lipid profiles, but reduced the development of atherosclerosis as detected by the elimination of local oxidative stress and reduced expression of monocyte chemoattractant protein-1 and platelet-derived growth factor. Azelnidipine also reduced the proliferation and migration of vascular smooth muscle cells in vitro. In atherosclerotic ApoE-knockout (ApoE-KO) mice fed a high cholesterol diet, azelnidipine but not amlodipine reduced the development of atherosclerosis. Neither drug changed the lipid profiles or systolic blood pressure of the mice. Thus, azelnidipine at clinically relevant doses exhibited anti-atherosclerotic effects in monkeys and mice independent of its blood pressure-lowering effects, suggesting that azelnidipine might be as a "vasculoprotective calcium channel blocker".

Keywords: Atherosclerosis; Calcium channel blockers; Cytokines; Smooth muscle cells; Azelnidipine

1. Introduction

Calcium channel blockers (CCBs) have been used worldwide to treat patients with hypertension and angina pectoris. Recent clinical trials with CCBs, such as PREVENT, ALLHAT, VALUE, CAPARES, ACTION, and CAMELOT, have provided evidence that reducing arterial blood pressure to close to normal ranges is of great importance for reducing cardiovascular events [1–6]. These clinical trials suggest that CCBs may have pleiotropic actions beyond simply lowering blood pressure. The pleiotropic actions of CCBs may be distinct from its pharmacologic actions related to blocking L-type calcium channels, but may be attributable to their lipophilic character, which gives them a high affinity for the membrane phospholipids of arterial wall cells, such as vascular smooth muscle cells (see review by Mason et al. [7]). CCBs' vasculoprotective actions include improvement of endothelial function, anti-inflammation effects, anti-oxidant effects, and anti-proliferation effects on vascular smooth muscle cells (VSMCs).

* Corresponding author at: Department of Cardiovascular Medicine, Graduate School of Medical Sciences, Kyushu University, 3-1-1 Maidashi, Higashi-ku, Fukuoka 812-8582, Japan. Tel.: +81 92 642 5358; fax: +81 92 642 5375.
E-mail address: egashira@cardiol.med.kyushu-u.ac.jp (K. Egashira).

0021-9150/$ – see front matter © 2007 Elsevier Ireland Ltd. All rights reserved.
doi:10.1016/j.atherosclerosis.2007.03.036

In animals, CCBs have been shown to prevent or attenuate atherosclerosis [8], hypertension-induced vascular remodeling, neointimal formation after vascular injury [9]. Azelnidipine is a newly developed third-generation CCB that has anti-hypertensive effects comparable to amlodipine [10]. Azelnidipine is strongly lipophilic and has a high affinity for membrane of vascular wall cells, such as vascular smooth muscle cells [11]. We recently reported that azelnidipine attenuated stent-associated neointimal formation associated with reduced expression of monocyte chemoattractant protein-1 (MCP-1) in non-human primates (cynomolgus monkeys) [12]. In that study, we found that azelnidipine's attenuation of neointimal formation was independent of its blood pressure-lowering actions in vivo, and that azelnidipine directly reduced MCP-1-induced proliferation of VSMC, suggesting that azelnidipine's beneficial effects on in-stent restenosis were mediated in part by direct inhibition of VSMC proliferation. However, the mechanisms of the anti-atherosclerotic action and the clinical significance of azelnidipine were not fully addressed.

The aim of this study is to investigate whether azelnidipine at clinically relevant doses attenuates atherosclerosis in non-human primates (cynomolgus monkeys) in ways that are independent of its blood pressure-lowering effects. To confirm the clinical significance of the findings, we used a non-human primate model of atherosclerosis [13]. Although it is difficult to choose an appropriate animal model for studying atherosclerosis, a non-human primate model may have an advantage over non-primate animal models, such as rabbits and mice: vascular inflammatory and proliferative responses to injury in non-human primates are presumed to be more similar to those in humans than are those of other non-primate animals. Therefore, the use of non-human primates may allow us to evaluate the efficacy of any therapies on atherosclerosis in clinically relevant conditions. Furthermore, to examine whether the observed anti-atherosclerotic effects are unique to azelnidipine or are a class-effect of CCBs, we also compared the effects of azelnidipine and amlodipine in ApoE-knockout (ApoE-KO) mice.

2. Methods

An enhanced Methods and Results section is available online at doi:10.1016/J.atherosclerosis.2007.03.036.

2.1. Cynomolgus monkeys: animals and study protocol

The study protocol was reviewed and approved by the Committee on the Ethics of Animal Experiments, Kyushu University Graduate School of Medical Sciences. Thirty-six 5-year-old male cynomolgus monkeys weighing 4.0 – 6.0 kg were purchased from Primate Ltd. (Gaoyao, Guang Dong, China). The monkeys were fed a high cholesterol diet (0.5% cholesterol and 6% corn oil) for 4 weeks prior to the balloon injury operation. Ticlopidine (100 mg) and aspirin (81 mg) were administered each day starting 7 days before the balloon procedure; ticlopidine was administered for 28 days, and aspirin was continued until euthanization at 6 months. The animals were randomized to 3 groups ($n = 12$ monkeys per group) as follows: (1) no treatment/vehicle control group (0.5% carboxymethyl cellulose sodium salt); (2) low-dose azelnidipine group (3 mg/kg per day; donated by Sankyo Pharmaceutical Co., Tokyo, Japan); and (3) high-dose azelnidipine group (10 mg/kg per day). These doses of azelnidipine were selected because we previously reported that first, the 3 and 10 mg/kg doses do not affect systemic arterial pressure and heart rate in conscious monkeys by telemetric measurements; and second, the low dose of azelnidipine used in the present study for monkeys was within clinical range, because the maximum drug concentration (C_{max}) of azelnidipine at 3 and 10 mg/kg per day was 36 ± 17 and 107 ± 17 ng/mL, respectively, in monkeys [12], while the C_{max} after oral administration of azelnidipine at 16 mg in hypertensive human subjects is reported to be 48 ± 19 ng/mL. Azelnidipine was administered to the monkeys once a day by gavage for 24 weeks. One week after starting azelnidipine treatment in the azelnidipine groups, all monkeys were anesthetized with ketamine hydrochloride (10 mg/kg IM) and sodium pentobarbital (30 mg/kg IV). The left femoral artery was surgically exposed, a 4 Fr sheath catheter was passed into the femoral artery, and monkeys received a balloon injury of the thoracic and abdominal aorta, as previously described [13]. The right femoral artery was then ligated and the incision was closed. After the operation, all monkeys were fed the same high cholesterol diet. Animal care before and after the operation took place in Gaoyao Kangda Laboratory Animal Science and Technology in China.

2.2. Comparison of azelnidipine and amlodipine in ApoE-KO mice

Male ApoE-KO mice were purchased from Jackson Laboratory (Bar Harbor, Maine, USA). ApoE-KO mice were fed a Western-type diet (Oriental Yeast, Tokyo, Japan) during the experiment. At 8 weeks of age, mice were randomly assigned into the following groups: (1) no treatment/vehicle control group ($n = 10$); (2) low-dose azelnidipine group (3 mg/kg per day; $n = 6$); (3) high-dose azelnidipine group (10 mg/kg per day; $n = 7$); and (4) amlodipine group (same class CCB; 10 mg/kg per day, donated by Pfizer Japan Inc., Tokyo, Japan; $n = 6$). Azelnidipine and amlodipine treatment was carried out for 8 weeks by mixing the drug with food for the mice. After 8 weeks of treatment, all mice were sacrificed and tissue was prepared for analysis. Tissue preparation was performed as previously described [14]. Briefly, after the mouse was killed, the aorta was rapidly removed from the left ventricle after perfusion with phosphate-buffered saline. The aorta from the arch to the bifurcation of the iliac artery was fixed in 10% buffered formalin for measurement of the surface area covered by lipid-staining lesions. To quantify the extent of the atherosclerotic lesions, adventitial tissue was removed from

the aortic arch and the aortic arch was opened longitudinally, stained with oil red O, and pinned out on a black wax surface. The percentage of the endothelial surface area stained by oil red O was determined [14].

Plasma total cholesterol, high-density lipoprotein cholesterol and triglycerides concentrations were determined using commercially available kits (Wako Pure Chemicals, Tokyo, Japan). Systolic blood pressure and heart rate were measured every other week (by the tail-cuff method [14]). Moreover, to evaluate the safety of azelnidipine, a multiplex immunoassay was performed using the Luminex Lab MAP instrument by Charles River Inc. (see online Supplementary data).

3. Results

3.1. Histopathological and immunohistochemical measurements in monkeys

In the thoracic aorta, treatment with low and high doses of azelnidipine significantly reduced the neointimal area (Fig. 1A and B; vehicle group: $1.86 \pm 0.23\,mm^2$, low-dose group: $0.96 \pm 0.16\,mm^2$, high-dose group: $1.02 \pm 0.19\,mm^2$). These doses also significantly reduced the intima-media ratio (Fig. 1B: vehicle group: 0.45 ± 0.26, low-dose group: 0.23 ± 0.04, high-dose group: $0.28 \pm$

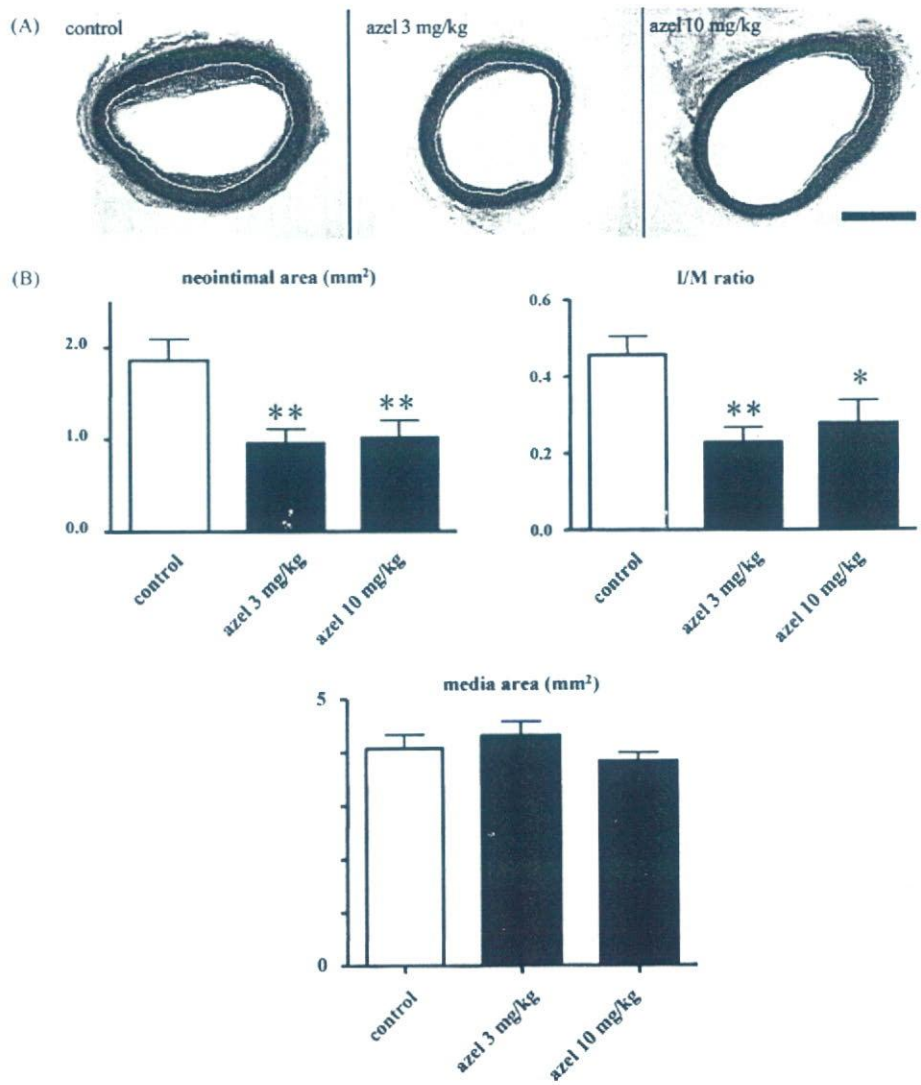

Fig. 1. Effects of azelnidipine on atherosclerosis in monkey thoracic aorta. (A) Representative photomicrographs are shown of Masson's trichrome-stained cross-sections of the injured thoracic aortas from the vehicle control group (control, left panel), low-dose azelnidipine group (azel 3 mg/kg, middle panel) and high-dose azelnidipine group (azel 10 mg/kg, right panel). Internal elastica lamina are outlined with white. Bar = 10 mm. (B) Measurements of the neointimal areas, intima/media (I/M) ratios, and media areas of the thoracic aortas from monkeys treated with or without azelnidipine as indicated ($n = 12$ each). $^*P < 0.05$, $^{**}P < 0.01$ versus vehicle control group. Each value represents mean ± S.E.M.

0.06). There was no difference in media area among the groups.

Immunohistochemical expression of MCP-1 and PDGF-BB and the composition of the neointima were then examined in the abdominal aorta in the neointima (Fig. 2A). Azelnidipine at low and high doses reduced PDGF-BB and MCP-1 expression in the neointima (Fig. 2). In contrast, neither dose of azelnidipine affected the neointimal area (vehicle group:

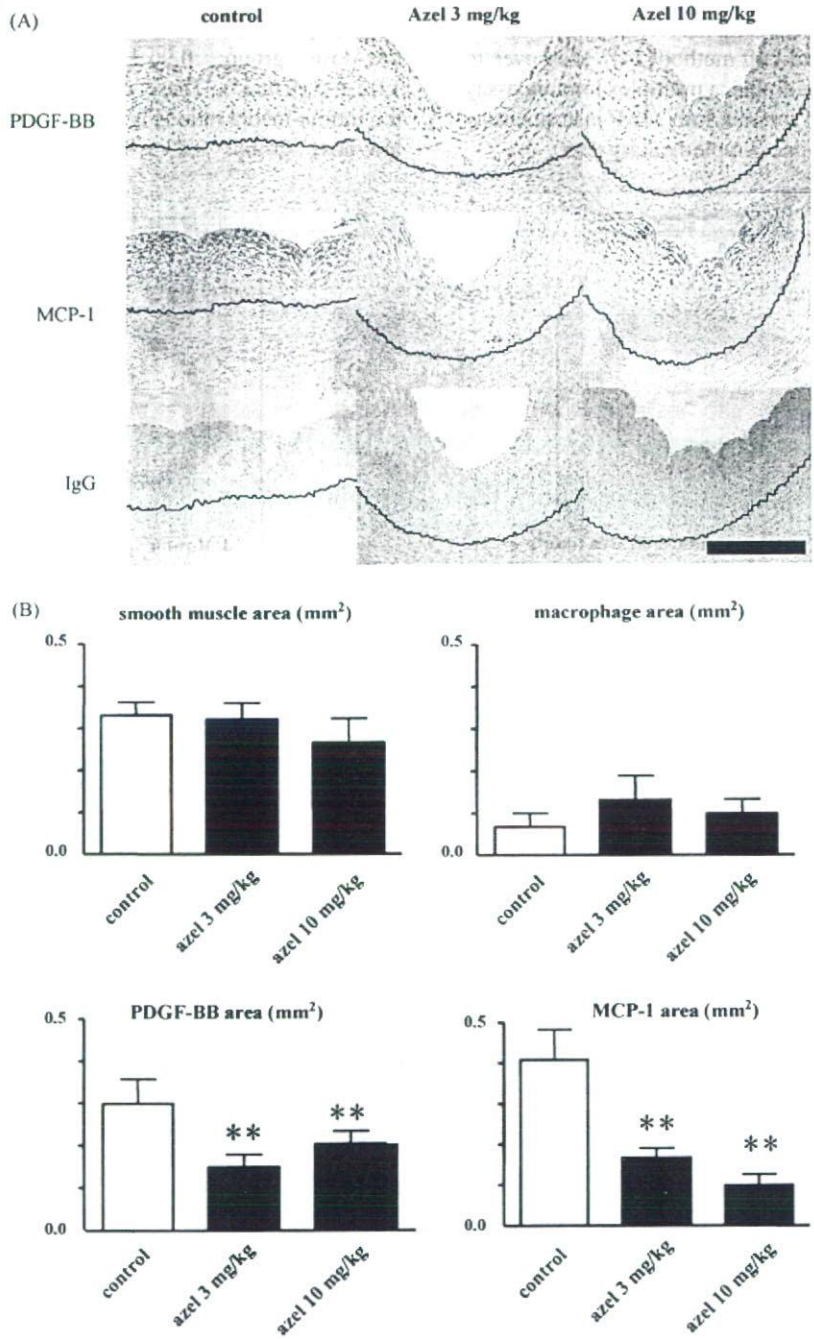

Fig. 2. Immunohistochemical detection of PDGF-BB and MCP-1 expression. (A) Cross-sections of abdominal aortas from experimental groups stained with the antibody against monocyte chemoattractant protein-1 (MCP-1), platelet-derived growth factor (PDGF), or non-immune IgG (negative control). Internal elastica lamina are outlined with blue. Bar = 100 μm. (B) The MCP-1- and PDGF-positive areas were markedly decreased in azelnidipine low- and high-dose groups. However, there were no significant differences in the smooth muscle cell areas and macrophage areas among the groups. $^{**}P < 0.01$ versus vehicle control group ($n = 12$ each). Each value represents mean ± S.E.M.

$1.49 \pm 0.10\,mm^2$, low-dose group: $1.54 \pm 0.15\,mm^2$, high-dose group, $1.27 \pm 0.17\,mm^2$) or the macrophage or smooth muscle areas (Fig. 2B).

3.2. Detection of local oxidative stress in the aorta using DHE staining

No DHE fluorescence was detected in the normal abdominal aorta (data not shown). As shown in Online Figure, the fluorescent signal attributable to superoxide production was markedly enhanced in the neointima and media from the control group. Azelnidipine at low and high doses eliminated the intensity of DHE fluorescence in the neointima (Online Figure), whereas the DHE signal intensity did not differ among three groups in the media (data not shown).

3.3. Proliferation and migration of vascular smooth muscle cells in vitro

Azelnidipine at 1, 10, and 100 nM significantly inhibited the PDGF-induced proliferation of the human coronary smooth muscle cells (Fig. 3A). To examine the effects of azelnidipine on the PDGF-induced release of MCP-1, MCP-1 concentrations in supernatant fluid were measured (Fig. 3B). PDGF increased the MCP-1 levels in supernatant from 462 ± 23 to 1322 ± 98 pg/mL. Azelnidipine at 1, 10, and 100 nM significantly reduced the MCP-1 levels to 548 ± 34, 742 ± 39, and 405 ± 33 pg/mL, respectively (Fig. 3B). Azelnidipine at 1, 10, and 100 nM also inhibited the PDGF-induced migration of rat aortic smooth muscle cells (Fig. 3C). The human coronary arterial smooth muscle cells treated with azelnidipine at 100 nM showed no signs of cell toxicity or apoptosis (data not shown).

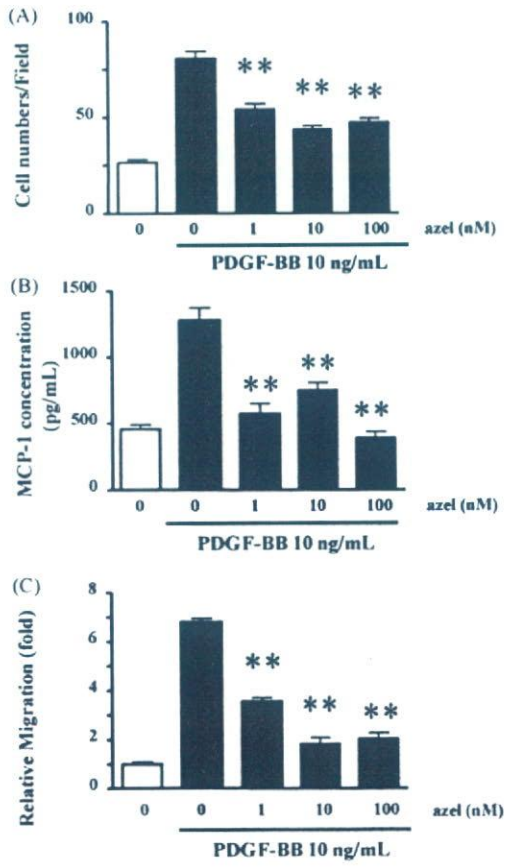

Fig. 3. Effects of azelnidipine on PDGF-induced proliferation of human coronary artery smooth muscle cells (A), on the concentration of MCP-1 in supernatant fluid from cell cultures treated with PDGF-BB (B), and on the migration of rat aortic smooth muscle cells (C). $^*P < 0.01$ versus control ($n = 9$). Each value represents mean ± S.E.M.

3.4. Comparison of azelnidipine and amlodipine in ApoE-KO mice

Azelnidipine at low and high doses markedly reduced atherosclerotic lesion formation as detected by staining of en face preparations of the aortas of ApoE-KO mice (Fig. 4).

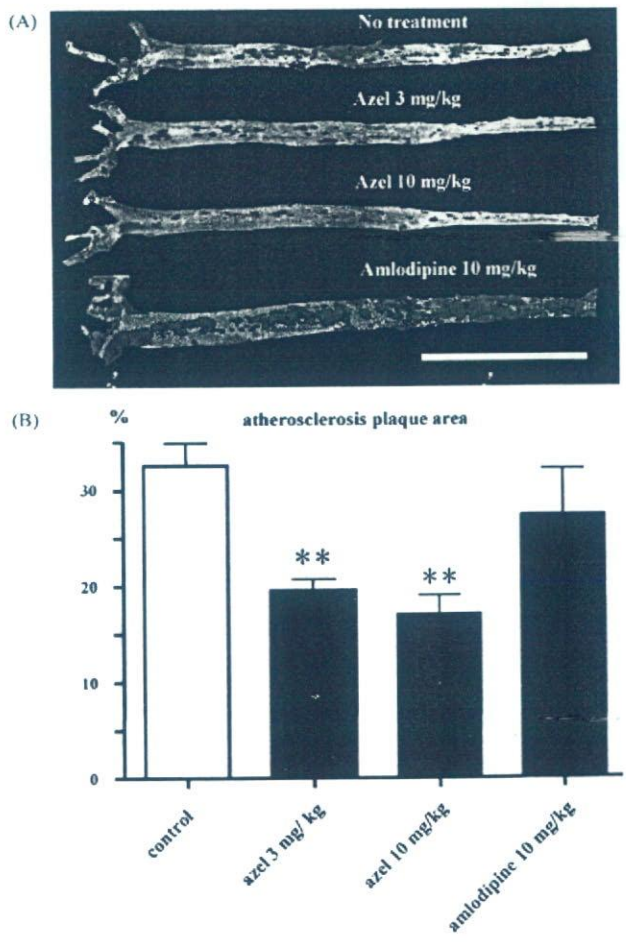

Fig. 4. Effects of azelnidipine and amlodipine on atherosclerosis in ApoE-KO mice. (A) En face preparations of aortas were stained with oil red O. Bar = 10 mm. (B) Quantitative comparison of atherosclerotic lesion size (percent of oil red O stained area) ($n = 6$–10). Data are reported as mean ± S.E.M. $^{**}P < 0.01$ versus no treatment group.